



Article

Hoof Impact and Foot-Off Accelerations in Galloping Thoroughbred Racehorses Trialling Eight Shoe–Surface Combinations

Kate Horan ^{1,*}, James Coburn ², Kieran Kourdache ³, Peter Day ¹, Henry Carnall ², Liam Brinkley ², Dan Harborne ², Lucy Hammond ³, Mick Peterson ⁴, Sean Millard ¹ and Thilo Pfau ^{1,5}

¹ Department of Clinical Science and Services, The Royal Veterinary College, Hawkshead Lane, Brookmans Park, Hertfordshire AL9 7TA, UK

² James Coburn AWCF Farriers Ltd., 8 Moulton Road, Newmarket CB8 8DU, UK

³ The British Racing School, Snailwell Road, Newmarket CB8 7NU, UK

⁴ Department of Biosystems and Agricultural Engineering, University of Kentucky, Lexington, KY 40506-0503, USA

⁵ Faculties of Kinesiology and Veterinary Medicine, University of Calgary, 2500 University Dr NW, Calgary, AB T2N 1N4, Canada

* Correspondence: khoran@rvc.ac.uk



Citation: Horan, K.; Coburn, J.; Kourdache, K.; Day, P.; Carnall, H.; Brinkley, L.; Harborne, D.; Hammond, L.; Peterson, M.; Millard, S.; et al. Hoof Impact and Foot-Off Accelerations in Galloping Thoroughbred Racehorses Trialling Eight Shoe–Surface Combinations. *Animals* **2022**, *12*, 2161. <https://doi.org/10.3390/ani12172161>

Academic Editor: Barbara Padalino

Received: 24 June 2022

Accepted: 19 August 2022

Published: 23 August 2022

Publisher's Note: MDPI stays neutral with regard to jurisdictional claims in published maps and institutional affiliations.



Copyright: © 2022 by the authors. Licensee MDPI, Basel, Switzerland. This article is an open access article distributed under the terms and conditions of the Creative Commons Attribution (CC BY) license (<https://creativecommons.org/licenses/by/4.0/>).

Simple Summary: To achieve optimal performance and low injury occurrence in horse racing, it is important to understand hoof–surface interactions. This study measured hoof accelerations in retired Thoroughbred racehorses as they galloped over turf and artificial surfaces in four shoeing conditions (aluminium, barefoot, steel and GluShu), using hoof-mounted accelerometers. During hoof landing, accelerations were increased for hindlimbs and leading limbs and on turf compared to the artificial surface. Barefoot hooves experienced the lowest impact accelerations and contrasted most with steel. During the propulsive stage of the stride, accelerations at “foot-off” were increased for low stride times, particularly in the hindlimbs, and on the artificial track. Increased impact accelerations on turf and in shod conditions could be detrimental to health and have implications for musculoskeletal injuries, whereas increased foot-off accelerations on the artificial surface may reflect this surface returning energy to the hoof and aiding propulsion, which could confer a performance benefit. Further work is needed to relate these findings to injury risk and racing outcomes specifically, particularly in racehorses galloping at top speeds.

Abstract: The athletic performance and safety of racehorses is influenced by hoof–surface interactions. This intervention study assessed the effect of eight horseshoe–surface combinations on hoof acceleration patterns at impact and foot-off in 13 galloping Thoroughbred racehorses retired from racing. Aluminium, barefoot, GluShu (aluminium–rubber composite) and steel shoeing conditions were trialled on turf and artificial (Martin Collins Activ-Track) surfaces. Shod conditions were applied across all four hooves. Tri-axial accelerometers (SlamStickX, range ± 500 g, sampling rate 5000 Hz) were attached to the dorsal hoof wall (x: medio-lateral, medial = positive; y: along dorsal hoof wall, proximal = positive; and z: perpendicular to hoof wall, dorsal = positive). Linear mixed models assessed whether surface, shoeing condition or stride time influenced maximum (most positive) or minimum (most negative) accelerations in x, y and z directions, using $\geq 40,691$ strides (significance at $p < 0.05$). Day and horse–rider pair were included as random factors, and stride time was included as a covariate. Collective mean accelerations across x, y and z axes were 22–98 g at impact and 17–89 g at foot-off. The mean stride time was 0.48 ± 0.07 s (mean ± 2 SD). Impact accelerations were larger on turf in all directions for forelimbs and hindlimbs ($p \leq 0.015$), with the exception of the forelimb z-minimum, and in absolute terms, maximum values were typically double the minimum values. The surface type affected all foot-off accelerations ($p \leq 0.022$), with the exception of the hindlimb x-maximum; for example, there was an average increase of 17% in z-maximum across limbs on the artificial track. The shoeing condition influenced all impact and foot-off accelerations in the forelimb and hindlimb datasets ($p \leq 0.024$), with the exception of the hindlimb impact y-maximum. Barefoot

hooves generally experienced the lowest accelerations. The stride time affected all impact and foot-off accelerations ($p < 0.001$). Identifying factors influencing hoof vibrations upon landing and hoof motion during propulsion bears implication for injury risk and racing outcomes.

Keywords: racehorse; hoof; acceleration; gallop; shoeing; surface; stride time

1. Introduction

Whole horse kinematics and injury mechanics are influenced by hoof–surface interactions. Establishing factors that control the timing and patterns of equine hoof motion throughout a stride cycle is necessary for optimising equine biomechanical function and performance, lessening the risk of injuries and enhancing economic gains. Thoroughbred racehorses galloping at high speeds during training and racing are particularly vulnerable to injuries [1–5]. As a result, the racing industry are placing increasing emphasis on understanding intrinsic and extrinsic factors that modulate a horse’s output on the track. This study focuses on the latter, and, in particular, seeks to better understand how the hoof kinematics of Thoroughbred racehorses relates to their shoeing condition and the ground surface they are travelling over at a range of gallop speeds.

Horses move asymmetrically over the course of a gallop stride cycle, so the sequence of footfalls influences the accelerations and loads experienced [6,7]. Hooves experience high deceleration and impact shock vibrations as they collide with the ground surface during galloping [8]. Impact-related shock is damped by the musculoskeletal structures of the limbs and hooves [9–11], and the associated vibrations may be quantified by accelerometers mounted to the hooves and/or the distal limbs [12–18]. The accelerations just before impact can be attributed to the variability in hoof position in preparation for contact with the ground surface [16]. Larger magnitude peaks are usually caused by the impact and hoof sliding and decelerating on the surface [19]. The sliding and/or sinking into the surface lowers the forces during deceleration [20,21] and reduces bending moments on the cannon bone [19]. The primary impact, or landing phase, for each hoof is followed by the secondary impact, during which time the hoof becomes largely fixed to the ground surface. The mass of the horse and jockey moves forward in the secondary impact, and although forces experienced by the limb in question are high, the hoof experiences minimum deceleration [8,13,22]. Each limb experiences peak vertical load as the horse transitions from braking to propulsion and its centre of mass is accelerated forward [23]. This stage is termed “mid-stance” and is a period of greater hoof stability [24]. After mid-stance, during propulsion, the heels of a hoof lift away from the surface and rotate through an angle of approximately 90 degrees about the toe, and the associated limb is gradually unloaded [8,25,26]. Finally, a limb will enter the swing phase. Hoof accelerations are, once again, high due to rapid hoof rotation as the joints of the digit flex and the limbs catch up and overtake the position of the upper body.

Micro-fractures in subchondral bone, cartilage breakdown and joint degeneration have been documented in response to hoof landing during locomotion [19,27–29]. Some injuries have been linked to the magnitude of impact forces and surface hardness [30,31]. This includes damage to the superficial digital flexor tendons in trotters through altered loading and joint kinematics [32,33] and osseous changes associated with high-frequency vibrations, which may ultimately result in lameness [34,35]. The influence of surface type on racing injuries, specifically, has been documented previously, but with conflicting results. A pooled analysis of multiple studies suggested that there were no differences in catastrophic musculoskeletal injuries between turf and all-weather or synthetic tracks, or turf and dirt tracks [1]. However, the nuances of individual racing settings may be an important consideration. For example, the competitive nature of the track, field size, distance and prize money all vary across racing settings [36]. It may also be important to consider front and hind limbs and lead versus non-lead limbs separately. For example, when turf,

synthetic and dirt tracks are compared, forelimb injuries are more common on dirt, whereas fatal hindlimb fractures are most likely to occur on turf; however, regardless of the surface, forelimbs are more likely to fracture [37]. Furthermore, surface conditions and composition must be considered; for example, temperature and moisture content influence properties such as firmness and cushioning [38–40]. Some research suggests that turf tracks that are faster increase the risk of fatal and non-fatal fractures and musculoskeletal injuries [2,41–49]. The type of injury is also a relevant consideration. For example, generally speaking, fatal and non-fatal fractures may be at a lower risk on synthetic tracks compared to turf and dirt [50]. However, the risk of biaxial proximal sesamoid bone fracture [51], fatal distal limb fracture [47,48] and lateral condylar fracture [52] may be increased on all-weather surfaces compared to turf.

Epidemiological evidence suggests that, in addition to surface conditions, certain types of horseshoes are associated with a higher risk of racehorse injury, and hence are a further key component of the hoof–surface interaction. For example, rim shoes that are similar to natural hoof shape may decrease injury risk [53], but some studies have associated toe grabs with injury occurrence [53–55]. In addition, the typically flat-foot, low-heel hoof conformation of racing Thoroughbreds [56,57] has been linked to injury [58–60], perhaps because these horses experience different foot mechanics to other horses [61,62]. However, limited data are available to understand the effect of different shoes on racehorse gait kinematics, and studies have, so far, tended to rely upon simulated conditions, such as treadmill work [63] or mechanical shoe-testing devices [64], with unclear representation to a horse racing on a track. This is in contrast to other equestrian disciplines where the influence of shoe shape, mass, composition and other modifications have been explored more readily [65–68]. This is likely a reflection on the tightly controlled shoeing conditions permitted by the racing industry [69]. However, our recent work assessing galloping racehorses in the field has alluded to the influence shoe–surface conditions have on both hoof breakover patterns [26] and upper body movements of horses and their jockeys [70]. Further work is needed to establish the impact of shoes and surfaces on racehorse gait kinematics and kinetics, including the accelerations and loads experienced. These findings are likely to have implications for the likelihood of horse and jockey injury and falls, as well as performance.

The aim of this study was to investigate the hoof accelerations of galloping Thoroughbreds trialling four different shoeing conditions at gallop on turf and artificial surfaces. We hypothesised that the magnitude of impact accelerations would increase on turf compared to the artificial surface, due to greater surface hardness. We also predicted that the harder the shoe composition, the higher the impact vibrations would be, and we expected shod conditions to be associated with higher impact accelerations compared to barefoot. We hypothesised that hoof accelerations would be higher at foot-off on the artificial track because breakover has previously been shown to be faster on this surface [26]. We also expected foot-off accelerations would be higher when the horses were barefoot, because unshod hooves should deform more readily upon impact and return greater energy to the hoof during propulsion.

2. Materials and Methods

2.1. Ethics

Ethical approval for this study was received from the RVC Clinical Research Ethical Review Board (URN 2018 1841-2). Informed consent was given by the jockeys, farriers and owners of the horses participating in this study.

2.2. Horse and Jockey Participants

Thirteen retired Thoroughbred horses in regular work and utilised for jockey education at the British Racing School (BRS) in Newmarket, UK, provided a convenience sample. All horses were considered sound by the jockey, farriers and BRS management prior to data collection. They ranged in age from 6 to 20 years old, had heights between 15.3 and

16.3 hh (1.6–1.7 m) and their masses, quantified using a weigh tape, ranged from 421 to 555 kg. Additional body dimensions, hoof morphometrics and shoe masses for the horses are reported in Reference [71]. Four jockeys participated in this study. One horse was ridden by two jockeys, giving rise to 14 horse–jockey pairs. The same horse-and-jockey pairings were used throughout this study, so the “horse–jockey combination” was fixed, while the shoe–surface condition varied. Unfortunately, not all horse–jockey pairings completed trials in all conditions for the following reasons: (1) turf access restrictions were occasionally imposed by the BRS when this surface was considered to be very hard; (2) two of the jockeys initially recruited for the study left the racing school or were injured and unavailable to complete data collection with the horse they had been paired with; and (3) one horse died, and another was placed on rest during the period of data collection, both for reasons unrelated to this study.

2.3. Trial Conditions

Horses underwent trials on an artificial (Martin Collins Activ-Track, Martin Collins Enterprises Berkshire, UK) and turf surface at the BRS in four shoeing conditions: aluminium raceplates (Kerckhaert Aluminium Kings Super Sound horseshoes, Stromsholm Limited, Milton Keynes, UK), barefoot, GluShu (aluminium–rubber composite shoes, Stromsholm Limited, Milton Keynes, UK) and steel shoes (Kerckhaert Steel Kings horseshoes, Stromsholm Limited, Milton Keynes, UK). The artificial track was a mixture of well-sorted quartz sand and CLOPF fibre, and it was wax-coated. The turf track was well-drained owing to the predominantly chalk lithology beneath. The surfaces and shoeing conditions tested were selected on the basis that they would develop understanding of the currently widely used training and racing options in the UK. In addition, we sought to investigate easily accessible yet novel shoeing options, which could be adopted by racehorse farriers, trainers and owners in the future. Horses’ hooves were trimmed prior to data collection and/or the application of shoes by the farriery team (JC, HC, LB or DH). All farriers followed the same trimming procedure set out by the lead farrier (JC). The order of trials for the eight possible shoe–surface combinations was randomized. The horses underwent a warm-up period in walk, trot, canter and gallop prior to data collection. Each data trial consisted of a minimum of two runs, to generate data for the horses galloping on both leads. However, some horses participated in additional runs if they struggled to achieve the desired lead, behaved unusually in a trial (such as bucking) or if equipment fell-off and needed to be reattached. Full weather data on and preceding data-collection days are available in Reference [71]. In summary, in the 72 h preceding and inclusive of data collection, mean temperature was 9.8 ± 2.3 °C (± 2 SE), mean rainfall was 0.2 ± 0.1 mm (± 2 SE) and mean humidity was $81.5 \pm 2.5\%$ (± 2 SE).

2.4. Equipment

Tri-axial accelerometers (SlamStick X, Mide Technology, United States), recording at a sample rate of 5000 Hz and with a measurement range of ± 500 g, were mounted to the dorsal hoof wall of each hoof in custom-made aluminium brackets (Figure 1). The brackets were glued to the hoof by using Superfast hoof adhesive (Vetec Royal Kerckhaert, The Netherlands). The accelerometers had in-built data loggers that were capable of recording continuously for up to 30 h, and their mass was 70 g. The x-axis of the accelerometers had a medio-lateral orientation (medial = positive), the y-axis was aligned along the hoof wall (proximal = positive) and the z-axis was in the dorso-palmar orientation (dorsal hoof wall = positive). Figure 1 illustrates the bracket design and accelerometer mounted to the hoof.

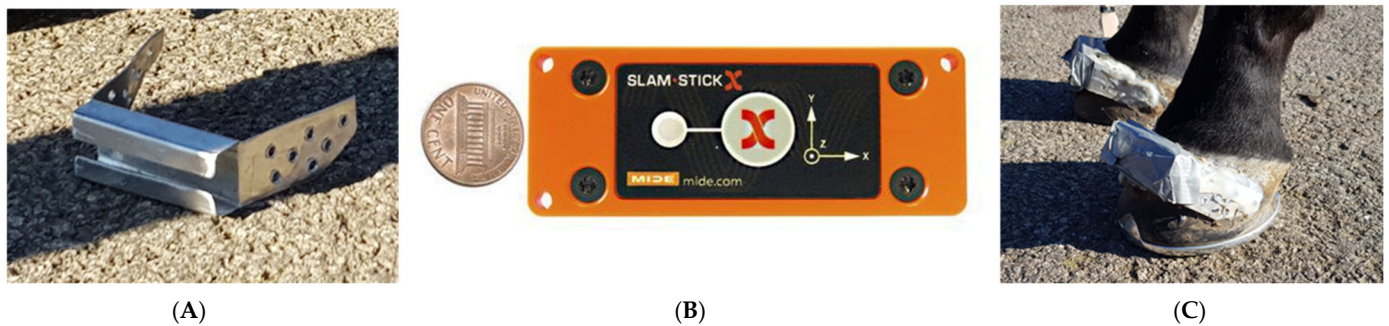


Figure 1. (A) Aluminium bracket. (B) Slamstick accelerometer. (C) Accelerometer and bracket system mounted to hoof.

2.5. Data Processing

Approximate timings of individual gallop runs were noted during data collection. These were used to identify relevant blocks of accelerometry data, and a custom-written MATLAB script was used to extract these data. A second custom-written MATLAB script associated with a GUI was then used to identify features of interest at hoof impact and foot-off. In summary, strides were selected manually from blocks of accelerometry data and then visually enlarged. The approximate positions of impact and foot-off (as indicated in Figure 2) for the strides were then clicked on manually. These positions were used in combination with a specified search window to identify the precise “minimum” (most negative) and “maximum” (most positive) values for the three acceleration axes at impact and foot-off. A second impact peak was used to define stride time. The size of the search window was adjusted manually to cover the same features of interest, regardless of stride duration, shoeing condition or surface. The impact was taken to encompass accelerations immediately before heel strike through to early stance. It could be readily identified from the data as being represented by acceleration spikes preceding flat traces. The flat traces were representative of stance and were followed by the foot-off acceleration spikes. Low accelerations were also associated with the swing phase, but these took place over a longer time period than stance, and the hoof was generally less stable. Data in the medio-lateral axis were inverted for the right fore and right hind to achieve a configuration with the medial direction as positive. The areas under the acceleration traces at set points forward and backward from the timing of the minimum and maximum were also quantified; these were defined both in time (± 5 ms, ± 10 ms, ± 15 ms and ± 20 ms) and by percentage through the stride ($\pm 1\%$, $\pm 2\%$, $\pm 3\%$, $\pm 4\%$, $\pm 5\%$). The areas reflected the change in velocity of the hoof in the period immediately prior to and post impact and foot-off. The data were grouped by horse, jockey, limb, shoeing condition, surface, gallop lead and gallop run. All data were processed by the same person (KH).

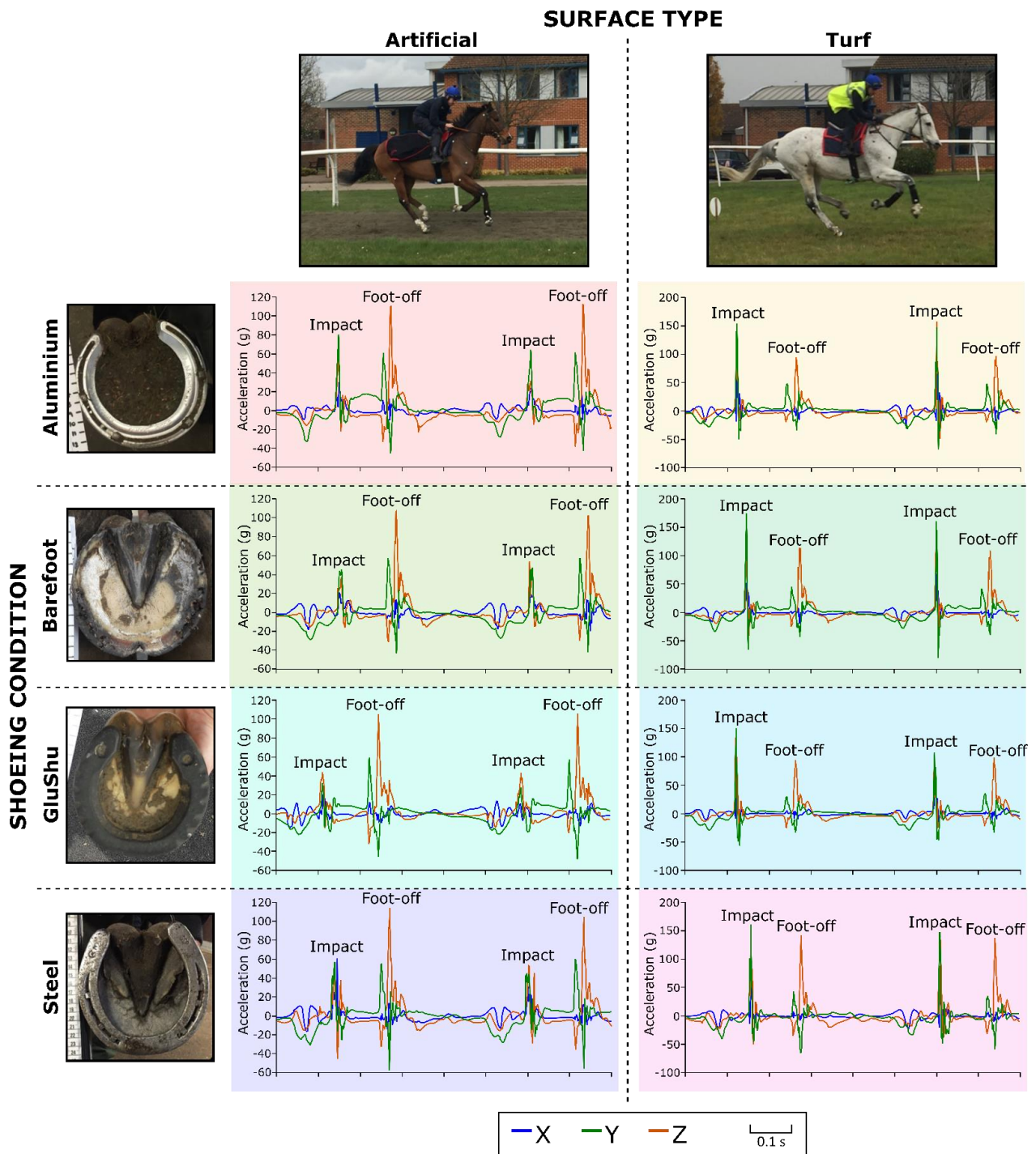


Figure 2. Examples of tri-axial accelerometry data collected from the hooves of the horse from horse-jockey combination 8 under the eight different shoe-surface combinations: x is medio-lateral, y is along the hoof wall proximo-distal and z is dorso-palmar.

A total of 41,183 strides were included in the analysis. Table 1 summarises the number available per shoe-surface combination for each horse-jockey pair.

Table 1. Number of strides analysed per shoe–surface combination for each horse–jockey pair. Please note that the horse–jockey ID numbers are consistent with References [26,70,71].

Horse–Jockey Pair ID	Shoe–Surface Combination							
	Aluminium– Artificial	Aluminium– Turf	Barefoot– Artificial	Barefoot–Turf	GluShu– Artificial	GluShu–Turf	Steel– Artificial	Steel–Turf
1	403	376	435	365	354	360	477	345
2	389	574	826	341				
3	903	379	465	582	332	307	670	811
4	397	411	332	378	386	552	291	537
5	776		655					
6	506		344		371	590	423	
7	210		627		409		249	
8	665	479	1054	339	315	664	684	449
9			443		533			
10	499	605	480	488	637	534	425	538
11	922	432	473	299	616	504	915	361
13	571	622	414	350	416	495	404	544
14	382	350	271	275	389	331	294	365
15			319	586			384	930

2.6. Statistics

Linear mixed models were implemented in SPSS to test for significant differences in tri-axial acceleration peaks and areas under peaks at both impact and foot-off, under the different shoe and surface conditions. Shoe, surface, stride time, “shoe*surface interaction”, “shoe*stride time interaction” and “surface*stride time interaction” were defined as fixed factors, and horse–rider pair and day were defined as random factors. Stride time was also included as a covariate. Histograms of models’ residuals were plotted, and normality was confirmed. The significance threshold in all statistical tests was set at $p < 0.05$. Models included data from all strides and a subset of the data for stride frequencies ≥ 2 Hz; 2 Hz is approximately equivalent to 9 ms^{-1} [72], which is a speed that is consistent with slow galloping speeds [73], and should exceed canter speeds of Thoroughbreds [63,74,75].

3. Results

3.1. Overview

We first present peak acceleration data for limbs independent of shoe–surface condition to assess the general patterns in the acceleration magnitudes per axis at impact and foot-off, independent of shoe or surface type (Table 2). Figure 2 illustrates example extracts of gallop strides per shoe–surface combination. The full raw dataset is available in the Supplementary Data File. It was apparent from the statistical models and a visual analysis of the minimum and maximum data using boxplots that differences between the entire dataset and the subset of data for stride frequencies ≥ 2 Hz were slight. Therefore, we focus on presenting and discussing the data from the entire dataset in the main manuscript but make all raw data and model significance results available in the Supplementary Data File.

To tackle the high volume of area data, a visual inspection using boxplots was helpful in identifying consistent trends amongst parameters. It was apparent that areas calculated for time windows extending further from the peaks had trends amongst shoe–surface conditions that were similar to those closer to the peaks. Therefore, we decided to focus on a short time window (5 ms), as this best represents the nature of the main peak (sharp or broad) immediately following impact or foot-off. In addition, although the data representing areas under minimum and maximum peaks were similar, it was decided that the areas under maximum peaks depicted clearer trends and were likely to be more informative because they are associated with the accelerations transferred into the hoof in the distal to proximal direction. We also considered area data after the main peaks to be of more relevance than those that preceded the main peaks. As such, we summarise results for area data at impact and foot-off in the 5 ms time window after the maximum in Appendix A (Figure A5) and include the linear mixed model results, along with the full dataset, in the Supplementary Data File.

Table 2. Summary of peak accelerations at impact and foot-off across the x, y and z acceleration axes for each of the limb types. Please note that, alongside the leading and non-leading limb data, “mixed lead” runs were included in the forelimb and hindlimb data outputs listed as “combined”.

Limb	Acceleration Parameter	Impact Mean (g)	2 SD	Foot-Off Mean (g)	2 SD	n	Mean Stride Time	2 SD
All limbs	X-maximum	44.16	67.85	16.55	20.65	41,183	2399.15	344.46
	X-minimum	−21.79	35.13	−17.17	17.85	41,183		
	Y-maximum	98.31	127.82	89.22	72.21	40,844		
	Y-minimum	−34.27	54.32	−38.11	44.08	40,844		
	Z-maximum	88.73	128.02	49.93	41.13	40,691		
	Z-minimum	−38.83	49.25	−30.46	39.28	40,691		
Combined Forelimb	X-maximum	36.96	47.27	14.57	18.60	20,882	2403.59	350.90
	X-minimum	−19.62	28.35	−17.26	18.47	20,882		
	Y-maximum	87.68	99.21	95.46	66.70	20,543		
	Y-minimum	−33.89	51.21	−34.88	36.67	20,543		
	Z-maximum	89.23	120.27	45.76	40.39	20,882		
	Z-minimum	−37.13	45.88	−28.97	42.96	20,882		
Leading Forelimb	X-maximum	42.38	49.43	14.61	20.08	8781	2411.34	334.76
	X-minimum	−20.72	31.83	−16.69	16.91	8781		
	Y-maximum	94.42	97.16	95.70	64.88	8633		
	Y-minimum	−36.57	51.39	−34.53	34.30	8633		
	Z-maximum	102.19	123.69	46.83	44.98	8781		
	Z-minimum	−35.39	38.42	−29.86	43.14	8781		
Non-Leading Forelimb	X-maximum	30.72	37.07	13.32	14.47	8641	2405.54	342.77
	X-minimum	−17.37	22.84	−17.33	19.64	8641		
	Y-maximum	78.00	83.84	91.63	63.04	8450		
	Y-minimum	−27.69	38.68	−32.79	31.60	8450		
	Z-maximum	67.93	85.40	43.83	36.58	8641		
	Z-minimum	−36.64	48.57	−27.94	41.75	8641		
Combined Hindlimb	X-maximum	51.56	81.29	18.58	21.84	20,301	2394.59	337.47
	X-minimum	−24.02	40.47	−17.09	17.19	20,301		
	Y-maximum	109.06	148.30	82.91	75.31	20,301		
	Y-minimum	−34.65	57.29	−41.38	49.64	20,301		
	Z-maximum	88.20	135.71	54.32	40.06	19,809		
	Z-minimum	−40.62	52.34	−32.03	34.71	19,809		
Leading Hindlimb	X-maximum	59.38	85.87	19.82	22.62	8719	2405.71	321.97
	X-minimum	−27.07	42.25	−16.27	17.18	8719		
	Y-maximum	123.44	150.61	77.82	72.50	8719		
	Y-minimum	−37.45	55.64	−39.76	46.93	8719		
	Z-maximum	98.53	120.37	51.75	36.95	8606		
	Z-minimum	−41.37	62.88	−30.21	35.67	8606		
Non-Leading Hindlimb	X-maximum	39.53	57.21	16.25	19.08	8384	2401.12	321.97
	X-minimum	−19.05	32.45	−17.20	14.84	8384		
	Y-maximum	87.07	120.04	83.80	67.21	8384		
	Y-minimum	−30.82	52.33	−40.37	45.89	8384		
	Z-maximum	65.58	89.33	55.99	40.33	8223		
	Z-minimum	−39.20	39.22	−33.47	32.39	8223		

3.2. Forelimbs

3.2.1. Impact

All significance values that were output from the linear mixed models are available in Supplementary Table S1. In summary, minimum and maximum impact accelerations for forelimbs were significantly affected by the shoe; surface; stride time; and interactions between shoe and surface, shoe and stride time and surface and stride time ($p \leq 0.003$). The exceptions were y-maximum, which was unaffected by a shoe*surface interaction ($p = 0.125$); and z-minimum, which was unaffected by the surface type ($p = 0.106$). Minimum and maximum accelerations for the leading forelimb were significantly affected by the shoe; surface; stride time; and interactions between shoe and surface, shoe and stride time and surface and stride time ($p \leq 0.027$). The exceptions were x-maximum, which was unaffected by a surface*stride time interaction ($p = 0.122$); and z-minimum, which was unaffected by either surface ($p = 0.083$) or a surface*stride time interaction ($p = 0.704$). Minimum and maximum accelerations for the non-leading forelimb were significantly affected by the shoe; surface; stride time; and interactions between shoe and surface, shoe and stride time and surface and stride time ($p \leq 0.035$). The exceptions were x-maximum, which was unaffected by a shoe*stride time interaction ($p = 0.052$) or a surface*stride time interaction ($p = 0.831$); x-minimum, which was unaffected by the surface*stride time ($p = 0.799$); y-minimum, which

was unaffected by the shoe ($p = 0.114$) and shoe*surface ($p = 0.094$); and z-minimum, which was unaffected by the surface ($p = 0.530$). Further details and comparisons amongst the shoe and surface conditions at impact are provided in Section 3.4, Section 3.5, Section 3.6

3.2.2. Foot-Off

The minimum and maximum foot-off accelerations for forelimbs were significantly affected by the shoe; surface; stride time; and interactions between shoe and surface, shoe and stride time and surface and stride time ($p \leq 0.024$). The exceptions were x-maximum, which was unaffected by shoe*stride time ($p = 0.082$); and y-minimum, which was unaffected by surface*stride time ($p = 0.102$). The minimum and maximum accelerations for the leading forelimb were significantly affected by the shoe; surface; stride time; and interactions between shoe and surface, shoe and stride time and surface and stride time ($p \leq 0.037$). The exceptions were x-maximum, which was unaffected by the surface ($p = 0.602$) or a surface*stride time interaction ($p = 0.424$); y-minimum, which was unaffected by the surface ($p = 0.170$); and z-maximum, which was unaffected by either shoe ($p = 0.072$) or a shoe*stride time interaction ($p = 0.243$). Minimum and maximum accelerations for the non-leading forelimb were significantly affected by the shoe; surface; stride time; and interactions between shoe and surface, shoe and stride time and surface and stride time ($p \leq 0.017$). This was true for all axis directions. Further details and comparisons amongst the shoe and surface conditions at foot-off are provided in Sections 3.4–3.6.

3.3. Hindlimbs

3.3.1. Impact

Minimum and maximum impact accelerations for hindlimbs were significantly affected by the shoe, surface, stride time, and interactions between shoe and surface, shoe and stride time and surface and stride time ($p \leq 0.048$). The exceptions were x-maximum, which was unaffected by a shoe*stride time interaction ($p = 0.053$); y-maximum, which was unaffected by the shoe ($p = 0.053$) or a shoe*stride interaction ($p = 0.184$). Minimum and maximum accelerations for the leading hindlimb were significantly affected by the shoe; surface; stride time; and interactions between shoe and surface, shoe and stride time and surface and stride time ($p \leq 0.029$). The exceptions were y-maximum, which was unaffected by a surface*stride time interaction ($p = 0.755$); y-minimum, which was unaffected by the surface ($p = 0.916$); z-maximum, which was unaffected by a surface*stride time interaction ($p = 0.962$); and z-minimum, which was unaffected by either shoe ($p = 0.145$) or a shoe*stride time interaction ($p = 0.067$). Minimum and maximum accelerations for the non-leading hindlimb were significantly affected by the shoe; surface; stride time, and interactions between shoe and surface, shoe and stride time and surface and stride time ($p \leq 0.028$). The exception was x-minimum, which was unaffected by a shoe ($p = 0.267$) or a shoe*stride time interaction ($p = 0.431$). Further details and comparisons amongst the shoe and surface conditions at impact are provided in Sections 3.4–3.6.

3.3.2. Foot-Off

Minimum and maximum foot-off accelerations for hindlimbs were significantly affected by the shoe; surface; stride time; and interactions between shoe and surface, shoe and stride time and surface and stride time ($p < 0.001$). The exception was x-maximum, which was unaffected by the surface ($p = 0.144$) or a surface*stride time interaction ($p = 0.288$). Minimum and maximum accelerations for the leading hindlimb were significantly affected by the shoe; surface; stride time; and interactions between shoe and surface, shoe and stride time, and surface and stride time ($p \leq 0.044$). The exception was x-maximum, which was unaffected by a shoe*stride time interaction ($p = 0.090$). Minimum and maximum accelerations for the non-leading hindlimb were significantly affected by the shoe; surface; stride time; and interactions between shoe and surface, shoe and stride time and surface and stride time (all $p \leq 0.047$). Further details and comparisons amongst the shoe and surface conditions at foot-off are provided in Sections 3.4–3.6.

3.4. Summary of Shoeing Condition Effect

3.4.1. Impact

The estimated marginal means (EMMs) for shoeing condition effects on impact are presented in Supplementary Table S2 and all post hoc pairwise comparisons (with Bonferroni correction) are provided in Supplementary Table S3. In each case, where EMM differences are reported below for pairwise comparisons, the first condition mentioned has the larger EMM value resulting in a positive difference.

The shoeing condition significantly influenced all impact accelerations in the forelimbs ($p \leq 0.026$), with the exception of y-minimum in the non-leading forelimb ($p = 0.114$). In the hindlimbs, the shoeing condition significantly influenced all impact accelerations ($p \leq 0.010$), with the exception of y-maximum for the combined dataset ($p = 0.053$); z-minimum in the leading hindlimb ($p = 0.145$) and x-minimum in the non-leading hindlimb ($p = 0.267$). The EMM impact accelerations were largest in terms of absolute magnitude for y-maximum in the leading hindlimb (mean of EMMs across shoeing conditions was 128.1 g), with the individual largest EMM acceleration of 142.7 ± 21.9 g (mean ± 2 SE in this section) being recorded for the y-maximum in the steel shoeing condition. For the y-maximum parameter, steel was most different to the barefoot condition particularly in the leading hindlimb (EMM difference = $\Delta 33.1 \pm 4.1$ g) (Supplementary Table S3). Mean impact maximum accelerations were 1.8–3.1 times larger than mean impact minimum accelerations, per axis direction. Y-maximum and z-maximum accelerations were of comparable magnitude and approximately double the magnitude of the x-maximum. The smallest accelerations, in terms of absolute magnitude, were recorded for the x-minimum in the non-leading forelimb (EMM average across shoeing conditions was 19.2 g), with the individual smallest absolute EMM acceleration of 16.2 ± 5.0 g being recorded for the x-minimum in the barefoot condition.

The largest impact acceleration offsets amongst shoeing conditions, in absolute terms, were most commonly observed between the steel and barefoot conditions (Supplementary Table S3): 11/18 comparisons in the forelimbs (combined forelimb data, leading forelimb and non-leading forelimb) and 6/18 comparisons in the hindlimbs (combined hindlimb data, leading hindlimb and non-leading hindlimb); for the six acceleration directions. Barefoot was amongst the pairwise comparisons with the largest offsets in 29/36 instances. Considering all six acceleration axes together in the individual limb datasets, the barefoot condition generated the lowest absolute means for EMM accelerations for all limbs: these ranged from 43.7 ± 20.8 g ($n = 6$) in the non-leading forelimb to 64.1 ± 30.8 g in the leading hindlimb. In contrast, the steel condition generated the highest absolute means for EMM accelerations for all limbs: these ranged from 53.1 ± 23.9 g in the non-leading forelimb to 74.2 ± 35.5 g in the leading hindlimb.

3.4.2. Foot-Off

The shoeing condition significantly influenced all foot-off accelerations in the forelimbs ($p \leq 0.024$), with the exception of z-maximum in the leading forelimb ($p = 0.072$). In the hindlimbs, the shoeing condition significantly influenced all foot-off accelerations ($p \leq 0.044$). The estimated marginal means (EMMs) for shoeing condition effects on foot-off are presented in Supplementary Table S2. The mean foot-off accelerations were largest in terms of absolute magnitude for y-maximum in the combined forelimb dataset (mean of EMMs across shoeing conditions was 95.6 g), with the individual largest EMM acceleration of 98.5 ± 11.2 g being recorded for the y-maximum in the GluShu shoeing condition for the leading forelimb; the subsequent three largest acceleration magnitudes were for the y-maximum in the steel condition (97.2 ± 11.2 g, 98.4 ± 9.8 g and 97.6 ± 10.7 g for the leading, non-leading and combined forelimb data, respectively) The smallest accelerations, in terms of absolute magnitude, were recorded for the x-maximum in the non-leading forelimb (mean across shoeing conditions was 13.7 g), with the individual smallest absolute EMM acceleration of 13.6 ± 2.3 g being recorded for the x-maximum in the GluShu condition for the non-leading forelimb. Noticeably, the y-maximum accelerations were considerably

larger than accelerations in the other axis directions: y-maximum accelerations were on average 5.4 times larger than x-axis accelerations, and 2.3 times larger than the y-minimum and z-axis accelerations. Nevertheless, pairwise comparisons between shoeing conditions only indicated a maximum difference of $\Delta 13.1 \pm 1.2$ g, which occurred between steel versus barefoot for the y-minimum parameter. The mean absolute difference between EMMs for pairwise shoe comparisons across all limbs was $\Delta 3.2 \pm 0.3$ g.

Considering all six acceleration axes together in the individual limb datasets, differences between conditions were small. Overall, the barefoot condition generated the lowest absolute means for EMM accelerations for all limbs: these ranged from 37.1 ± 23.9 and 37.1 ± 19.5 g ($n = 6$) in the non-leading forelimb and the leading hindlimb, respectively, to 37.3 ± 23.7 g in the leading forelimb and 39.1 ± 21.6 g in the leading hindlimb. In contrast, the steel condition generated the highest absolute means for EMM accelerations for all limbs: these ranged from 40.2 ± 25.2 g in the non-leading forelimb to 43.8 ± 23.2 g in the non-leading hindlimb. However, it is important to note that the results showed a dependency on stride time (Section 3.7).

3.5. Summary of Surface Effect

3.5.1. Impact

The surface type significantly influenced all impact accelerations in the forelimbs ($p \leq 0.013$), with the exception of z-minimum ($p = 0.106$ for the combined forelimb data, $p = 0.083$ for the leading forelimb and $p = 0.530$ for the non-leading forelimb). In the hindlimbs, surface significantly affected all impact accelerations ($p \leq 0.015$), with the exception of y-minimum ($p = 0.916$) in the leading hindlimb. All EMMs for surface effects on impact are presented in Supplementary Table S4 and the post hoc results for pairwise artificial–turf comparisons are presented in Supplementary Table S5. Surface effects were clearly apparent across all acceleration axes (Figure 3; Figure A1). Impact accelerations were always larger on turf in all directions for forelimbs and hindlimbs. Of note, the z-maximum and y-maximum provoked the highest accelerations. The highest EMM acceleration was recorded on turf for y-maximum in the leading hindlimb (167.1 ± 21.8 g; mean ± 2 SE in this section), while the lowest was observed for the x-minimum on the artificial in the non-leading forelimb (15.0 ± 5.0 g). The greatest contrast was present for the y-maximum in the leading hindlimb; EMM y-maximum acceleration was $\Delta 78.1 \pm 3.6$ g higher on turf compared to the artificial surface. The largest difference in absolute terms for the forelimbs occurred for the leading forelimb ($\Delta 60.7 \pm 2.8$ g) for the z-maximum parameter.

Considering all six acceleration axes together in the individual limb datasets, the absolute means of EMM accelerations on the artificial surface ranged from 36.4 ± 15.7 g ($n = 6$) in the non-leading forelimb to 49.5 ± 23.8 g in the leading hindlimb. In contrast, absolute means for EMM accelerations on turf ranged from 59.8 ± 28.6 g in the non-leading forelimb to 87.7 ± 41.5 g in the leading hindlimb.

3.5.2. Foot-Off

The surface type significantly influenced all foot-off accelerations in the forelimbs ($p \leq 0.022$), with the exception of x-maximum ($p = 0.602$) and y-minimum ($p = 0.170$) in the leading forelimb. In the hindlimbs, surface type significantly affected all foot-off accelerations ($p \leq 0.047$), with the exception of x-maximum ($p = 0.144$) in combined hindlimb data. The EMMs for surface effects on foot-off are presented in Supplementary Table S4. Foot-off accelerations were nearly always greater on the artificial surface, with the exceptions being x-minimum and y-minimum in the non-leading forelimb; x-minimum in the leading hindlimb; and x-maximum and y-minimum in the non-leading hindlimb. As observed amongst the shoeing condition effects, the y-maximum accelerations were noticeably larger than accelerations in the other directions: here, y-maximum accelerations were, on average, 5.0 times larger than x-axis accelerations and 2.3 times larger than the y-minimum, z-minimum and z-maximum accelerations. However, it was again the z-maximum—in this case, for the leading forelimb—which displayed the greatest contrast

($\Delta 12.6 \pm 1.2$ g) between turf and artificial surfaces (Supplementary Table S5). On average, for forelimbs, the z-maximum accelerations were 25% higher on turf, and this compared to an increase of 9% on turf for hindlimbs

Considering all six acceleration axes together in the individual limb datasets, the absolute means of EMM accelerations on the artificial surface ranged from 40.3 ± 25.3 g for the non-leading forelimb to 42.2 ± 25.7 g in the leading forelimb. Absolute means for EMM accelerations on turf ranged from 37.2 ± 22.6 g in the leading forelimb and 37.2 ± 22.5 g in the non-leading forelimb to 40.8 ± 21.0 g in the non-leading hindlimb. These data therefore indicate that the accelerations on turf at foot-off were reduced relative to the artificial surface, in contrast to the impact data where the reverse was true. Specifically, accelerations were up to 33% greater on the artificial surface compared to the turf for forelimbs and up to 20% greater in the hindlimbs.

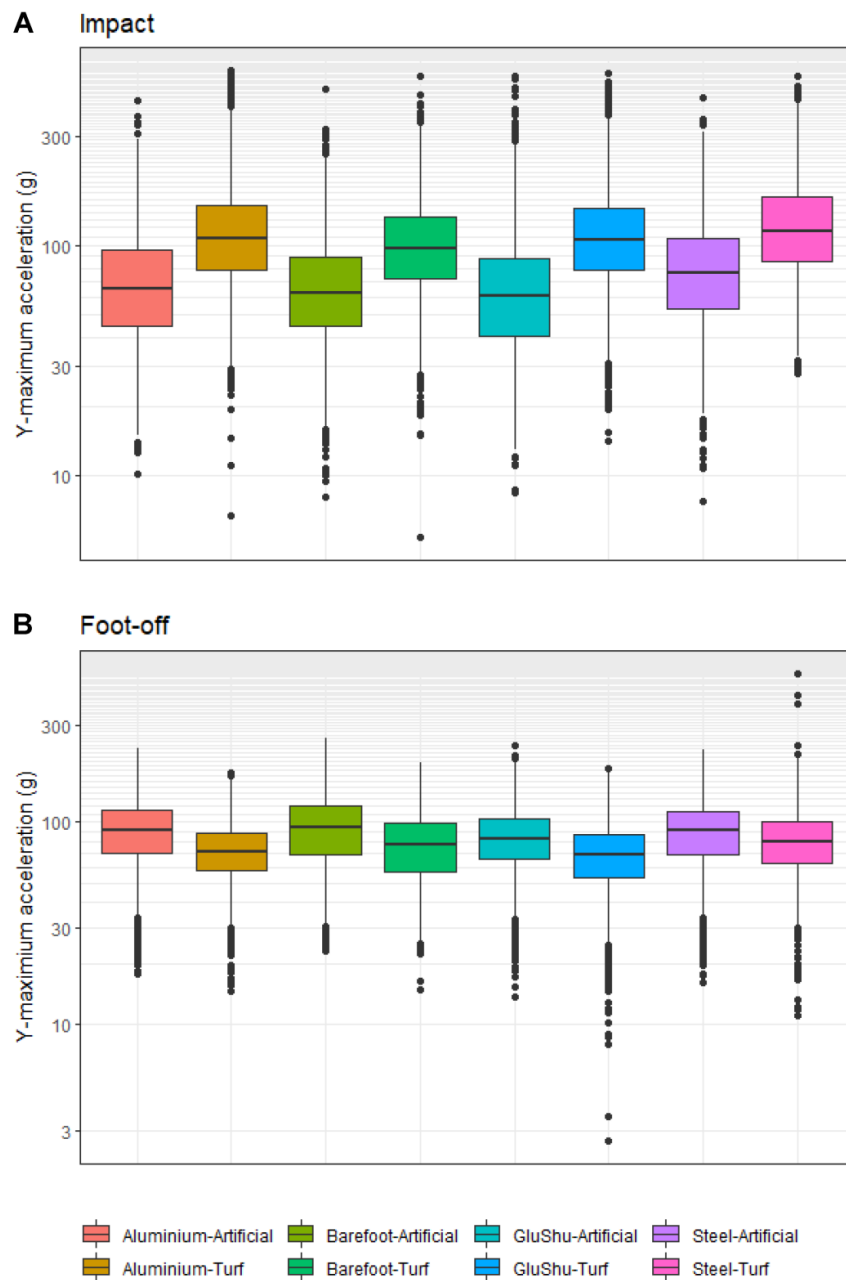


Figure 3. (A) Boxplots illustrating the impact accelerations for the y-maximum parameter across shoe–surface combinations. (B) Boxplots illustrating the foot-off accelerations for the y-maximum parameter across shoe–surface combinations. Data are pooled across limbs in each case.

3.6. Shoe–Surface Interactions

The EMMs for shoe–surface combinations are presented in Supplementary Table S6. Post hoc tests were run on acceleration parameters that indicated a significant shoe–surface interaction. As the y-maximum parameter seemed to be particularly sensitive to shoe and surface effects (Sections 3.4 and 3.5) and often recorded the highest peak accelerations, we focus on outlining the results from this parameter. This is also the parameter most strongly correlated to stride time at foot-off (Appendix A Figure A3). However, the full output of this post hoc analysis for all acceleration parameters is provided in Supplementary Table S7. In each case, where EMM differences are reported below for pairwise comparisons, the first condition mentioned has the larger EMM value, resulting in a positive difference. Please note that values reported below, in the shoe–surface comparisons, are from the post hoc models (Supplementary Table S7) and, hence, differ slightly from those from the initial models (Supplementary Table S6).

3.6.1. Impact

The y-maximum data for the leading forelimb indicated that the greatest EMM difference of $\Delta 72.8 \pm 3.8$ g (mean ± 2 SE in this section) was observed between the aluminium–turf and barefoot–artificial conditions. However, this was closely followed by the comparison between the steel–turf and barefoot–artificial conditions, which had an EMM difference of $\Delta 71.4 \pm 3.9$ g. The only pairwise comparisons that were not significantly different were aluminium–artificial versus GluShu–artificial, aluminium–turf versus steel–turf and barefoot–turf versus GluShu–Turf ($p = 1.0$ in each case).

For the non-leading forelimb, the magnitudes of EMM differences were smaller. Specifically, the largest EMM difference between the steel–turf and barefoot–artificial was $\Delta 64.3 \pm 3.3$ g, which was followed by the comparison between the steel–turf versus aluminium–artificial (EMM difference = $\Delta 58.6 \pm 3.5$ g) and GluShu–turf versus barefoot–artificial (EMM difference = $\Delta 58.4 \pm 3.4$ g). Only the aluminium–artificial and GluShu–artificial combinations were not significantly different ($p = 0.166$). Please note that the combined forelimb data were not significantly affected by a shoe–surface interaction (Supplementary Table S1), so the offsets amongst shoe–surface conditions are not reported here.

The y-maximum data for the hindlimbs indicated that larger acceleration differences were at play amongst the shoe–surface combinations, relative to the forelimb data. For the combined hindlimb data, the EMM differences between the aluminium–turf versus barefoot–artificial and the GluShu–turf versus barefoot–artificial, each of $\Delta 89.0$ g, were the largest, followed by steel–turf versus barefoot–artificial, which had an EMM difference of $\Delta 87.1 \pm 3.8$ g. There were four pairwise comparisons that were not significantly different: aluminium–artificial versus GluShu–artificial; aluminium–turf versus GluShu–turf; aluminium–turf versus steel–turf; and GluShu–turf versus steel–turf (all $p = 1.0$). All other comparisons for the combined hindlimb data were significant ($p \leq 0.006$).

For the leading hindlimb, peak EMM acceleration differences reached $\Delta 110.0 \pm 5.7$ g for the steel–turf versus barefoot–artificial condition, closely followed by GluShu–turf versus barefoot–artificial (EMM difference = $\Delta 99.6 \pm 6.0$ g) and steel–turf versus aluminium–artificial (EMM difference = $\Delta 99.4 \pm 6.1$ g). In contrast, the aluminium–turf versus GluShu–turf comparison indicated no significant difference ($p = 1.0$), and the GluShu–artificial and steel–artificial were also not significantly different ($p = 0.104$); all other comparisons highlighted significant differences ($p \leq 0.007$).

The non-leading hindlimb data indicated that GluShu–turf versus barefoot–artificial was most different (EMM difference of $\Delta 75.8 \pm 5.2$ g), followed by aluminium–turf versus barefoot–artificial ($\Delta 72.8 \pm 4.8$ g) and steel–turf versus barefoot–artificial ($\Delta 68.3 \pm 4.8$ g). The data therefore show that differences amongst shoe–surface conditions were greater in the leading limbs, for both hindlimbs and forelimbs. For the non-leading hindlimb, there were four non-significantly different conditions: aluminium–artificial versus GluShu–artificial; aluminium–turf versus GluShu–turf; aluminium–turf versus steel–turf; and

GluShu–artificial versus steel–artificial (all $p = 1.0$). All other comparisons were significant ($p \leq 0.029$).

3.6.2. Foot-Off

Accelerations at foot-off had smaller absolute magnitudes for EMM differences amongst shoe–surface combinations. For the combined forelimbs, the largest EMM difference of $\Delta 11.1 \pm 1.5$ g was observed between the GluShu–artificial versus aluminium–turf, closely followed by the GluShu–artificial versus GluShu–turf (EMM difference = $\Delta 10.7 \pm 1.3$ g) and the steel–artificial versus aluminium–turf (EMM difference = $\Delta 10.2 \pm 1.4$ g). Only the aluminium–artificial versus barefoot–artificial, aluminium–turf versus GluShu–turf, barefoot–turf versus steel–turf and GluShu–artificial versus steel–artificial conditions were not significantly different (each with $p = 1.00$); all other pairwise comparisons were significant, with p -values < 0.001 .

For the leading forelimb, there were eight EMM differences with magnitudes exceeding $\Delta 10$ g. The largest differences were between GluShu–artificial and aluminium–turf ($\Delta 17.3 \pm 2.0$ g), followed by GluShu–artificial versus barefoot–turf ($\Delta 15.4 \pm 2.2$ g) and steel–artificial versus aluminium–turf ($\Delta 14.4 \pm 2.0$ g). The following pairwise comparisons were not statistically different: aluminium–artificial versus barefoot–artificial ($p = 1.00$), aluminium–turf versus barefoot–turf ($p = 1.00$), barefoot–turf versus steel–turf ($p = 0.375$) and GluShu–turf versus steel–turf ($p = 1.00$); all other comparisons had p -values ≤ 0.049 .

For the non-leading forelimb, the GluShu–artificial versus GluShu–turf and steel–artificial versus GluShu–turf comparisons, each had differences of $\Delta 13.9$ g. They were followed in magnitude by the barefoot–artificial versus GluShu–turf EMM difference ($\Delta 12.4 \pm 2.0$ g). For this limb, there were seven pairwise shoe–surface comparisons that were not significantly different ($p \geq 0.084$).

Amongst the combined hindlimb data, differences amongst conditions were comparable to the forelimb data. The largest EMM difference was for the barefoot–turf versus GluShu–turf ($\Delta 12.5 \pm 1.5$ g), followed by the steel–artificial versus GluShu–turf ($\Delta 11.6 \pm 1.5$ g). All other EMM differences were less than $\Delta 10$ g, and eight of these were non-significant ($p = 1.00$).

EMM differences in the leading hindlimb were largest between the steel–artificial and GluShu–turf conditions at $\Delta 16.9 \pm 2.1$ g. This was followed by the EMM differences between steel–artificial and aluminium–turf ($\Delta 13.9 \pm 2.1$ g) and steel–artificial versus steel–turf ($\Delta 13.8 \pm 2.0$ g). Here, there were more comparisons that were not significantly different; the p -values for 11 comparisons were ≥ 0.095 .

3.7. Stride Time

Impact accelerations for all axes showed weak negative correlations with stride time. There were moderate correlations between stride time and foot-off accelerations, in particular for the y-maximum and z-maximum parameters. Figure 4 summarises data for the y-maximum acceleration parameter, subdivided according to shoe–surface combination (using the full dataset for forelimbs and hindlimbs). These trends are further illustrated in Appendix A Figure A4, where the strength of the correlations and significance values are also indicated per limb type for all acceleration axes.

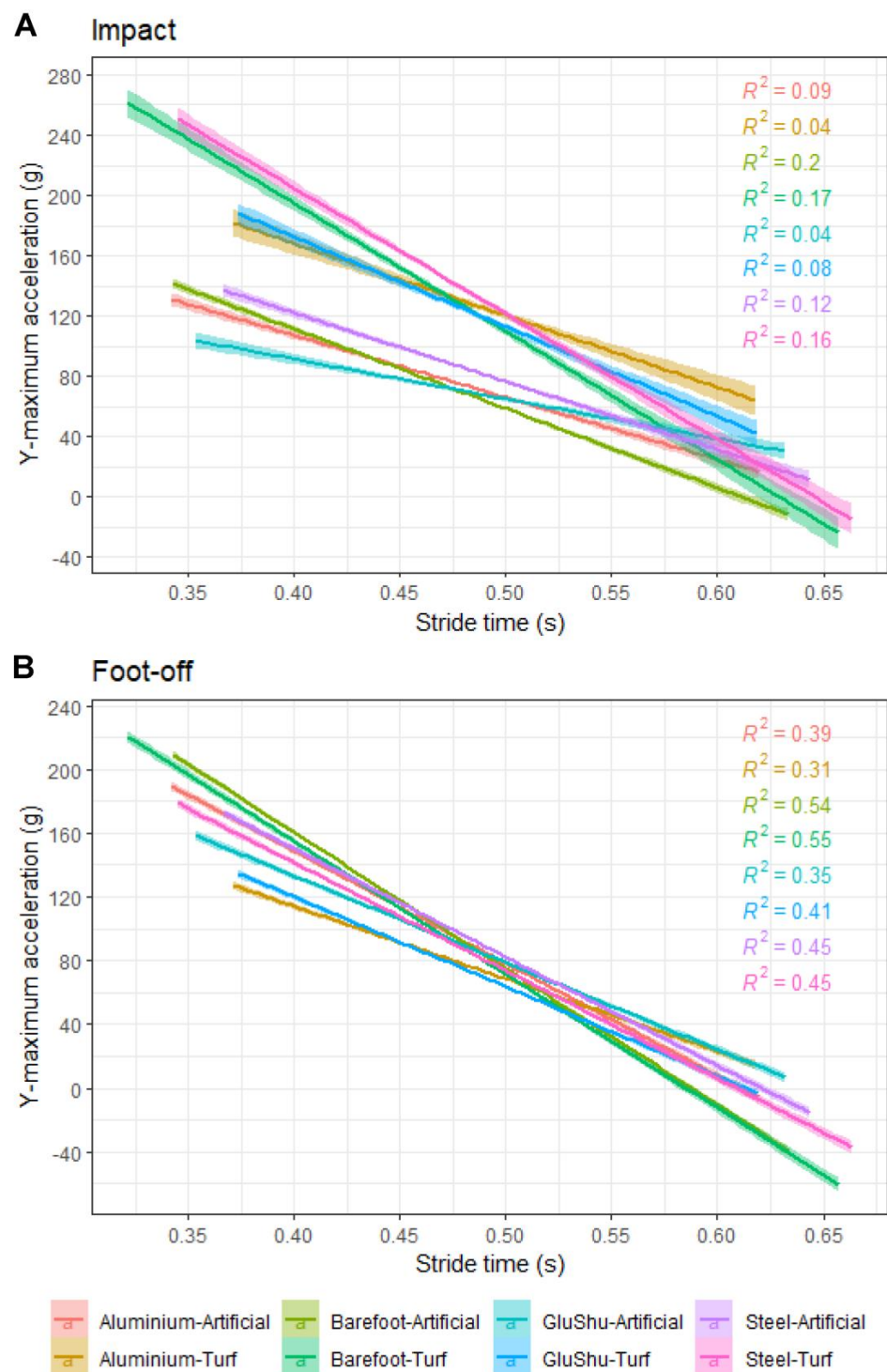


Figure 4. Relationship between hoof accelerations and stride time for the y-maximum parameter at (A) impact and (B) foot-off, subdivided by the shoe-surface combination for the entire dataset. The r^2 values for the linear regressions are indicated. All $p < 0.001$.

4. Discussion

Identifying factors that influence the accelerations experienced by a horse's hoof during landing and take-off bears implication for the injury risk and performance of racehorses and jockeys on the racetrack. Although epidemiological evidence indicates that multiple factors are associated with injury risk, including horse characteristics (age, sex and performance quality), training and racing history, pre-existing injuries and race

characteristics (e.g., geometry and class), the ground-surface conditions and hoof-shoeing conditions are factors that may be managed relatively easily and offer practical solutions to improve racing outcomes. This study emphasised the important influence that ground-surface type and shoeing condition have on tri-axial accelerations experienced at the dorsal hoof wall.

4.1. Impact

The data presented indicated that the hoof accelerations experienced at impact were 1.4–1.9 times and 1.2–2.4 times greater on turf compared to the artificial track for the forelimbs and hindlimbs, respectively. This trend toward higher accelerations on turf than synthetic surfaces is consistent with previous studies comparing hoof impact variations on turf versus synthetic surfaces at the trot and canter [16]. The acceleration power and frequency of hoof wall vibrations have previously been linked to surface hardness [13,16,21,76–78]. It is likely that the results here reflect the greater hardness of the turf compared to the artificial surface, even under the turf conditions studied, which were deemed “soft” to “good to firm”. This is important to recognise, as track hardness appears to be related to racing injuries [31,79]. The artificial surface was probably better at damping impact accelerations and provided greater cushioning to the hoof upon landing, despite this not being perceivable by the jockeys [71]. This interpretation is consistent with previous studies, which have demonstrated that synthetic surfaces have a higher damping capacity and lead to reduced hoof vibrations upon landing than turf, dirt and crushed sand [16,17,80].

The smallest relative difference between surfaces was observed for the z-minimum in all limbs, although this parameter was the most difficult to target consistently during data processing. For the forelimbs, the y-maximum and z-maximum showed the largest relative differences between surfaces (all 1.7–1.9 times larger on turf). In the hindlimbs, the greatest relative difference between surfaces was apparent for the y-minimum (2.2–2.4 times greater on turf); however, as noted in the Results section, the largest absolute difference between surfaces was 78.1 g for the y-maximum parameter in the leading hindlimb. The differing sensitivity of the six acceleration axes to surface type between forelimbs and hindlimbs may indicate that the hoof orientation on and immediately after landing is consistently different between the forelimbs and hindlimbs. For example, it would make sense for the accelerations represented by z-maximum (in the dorsal direction of the hoof) to be most closely associated with horizontal braking. Forelimbs are responsible for decelerating the horse in each stride cycle [22,81,82], and it is therefore logical that the z-maximum parameter would have greater sensitivity to the surface type in forelimbs. In addition, the forelimb hooves may have a greater tendency to land obliquely, whereas it is possible that the hindlimb hooves adopt an orientation on landing whereby the solar surface is closer to a parallel orientation to the ground surface, which could explain the particular sensitivity of the hindlimb y-axis data to surface condition.

Previous studies have indicated that the right hindlimb on a counter-clockwise track (this would be the non-leading hindlimb) has an overall higher incidence of fracture than the left hindlimb, but it shows no difference in injury risk due to surface type [37]. In addition, previous comparisons between contralateral and ipsilateral pairs of limbs found that the leading forelimb and non-leading hindlimb were at greater risk [37]. Data from this study suggest that the leading limbs experience the largest accelerations on the tracks used here, which had only a very slight anticlockwise bend [70]. Based on the EMMs for surface effects (Supplementary Table S4) averaged across all acceleration axes, the leading limbs had accelerations that were 1.5 times larger than the non-leading limbs. This could make them more vulnerable to injury, as high accelerations reflect more rapid loading during the secondary impact phase of the stride cycle, and previous work has found a relationship between impact forces and lameness [30]. Comparing the impact data across all stride times, it is suggested from our data that, at low stride times (i.e., higher speeds), the accelerations in the dorso-palmar (especially z-maximum) direction are proportionally larger for the leading limbs (Appendix A Figure A4). This could suggest that the hoof landing patterns

are also dependent on speed and may reflect the reduced overlap between individual limb-stance phases at higher gallop speeds [72]. During impact, the y-axis data (along the hoof wall) are probably most closely related to the ground reaction force, and this may explain why the accelerations were often large along this axis and why the y-maximum parameter appeared to be particularly sensitive to shoe–surface conditions. Moreover, at higher gallop speeds, it is plausible that there is proportionally greater hindlimb loading [26], and this may also help to explain why the y-minimum EMMs showed the largest proportional differences between surfaces for hindlimbs when assessing the data as a whole.

When all acceleration axes were considered together, the data indicated that impact acceleration peaks were 7–12% higher in aluminium shoes, 2–8% higher in GluShus and 10–18% higher in steel shoes when compared to the barefoot condition (comparisons made in the individual limbs). This compares to a previously reported difference of 15% between shod and unshod horses during simulated impact loading at trot in an in-vitro model [11]. However, accelerations were up to 25–30% higher in steel shoes compared to barefoot for the y-minimum and x-minimum parameters. The higher accelerations typically associated with the steel shoeing condition at impact may reflect the high rigidity and relative hardness of steel [83], which would have initiated rapid energy loss through hoof and limb vibrations. Shoeing with steel shoes has also been found to increase the maximal vertical force compared to barefoot in trotting Warmblood horses [84]. In contrast, the greater similarity in accelerations for GluShu relative to barefoot probably reflects greater damping in this condition due to the rubber coating on the shoe. Some previous work has also found synthetic polyurethane shoes and pads made of synthetic rubber can reduce peak impact vibrations in trotting horses [12,85], although no differences amongst shoeing conditions with and without a pad and packing material were found in an in vitro model [86]. The hoof was perhaps most efficient at energy absorption on landing when barefoot because the tubules embedded in the inter-tubular matrix were better able to dissipate energy through cracking and deformation while protecting the matrix from fracture or damage [87]. Unshod feet are known to undergo a greater degree of heel expansion, and this movement could help to dissipate the impact vibrations [88]. In addition, because the barefoot sole is closer to the ground surface compared to a shod foot, the frog and solear surface participate in the impact sooner than in the shod conditions, and the load will be more readily distributed over the full area of the solear surface [89]; an effect that is also likely to reduce the frequency of the vibrations measured at the dorsal hoof wall. When combined with the artificial surface, it is therefore unsurprising that the barefoot hooves usually experienced the lowest impact accelerations and typically contrasted most with steel shod hooves on turf. These findings tie in with the horses' and jockeys' centre-of-mass displacements. The largest vertical centre of mass displacement differences were also present between barefoot–artificial and steel–turf conditions [70], suggesting that the patterns in hoof kinematics may be translated into upper-body kinematics.

Further work is needed to establish the relative risk of damage to the hoof and more proximal limb structures in association with the observed variability in accelerations amongst barefoot and shod conditions at gallop. It will be important to establish whether there are certain thresholds for impact accelerations that may be conducive to the development of injuries or pathologies, such as osteoarthritis. Performance implications are also key. Previous work has suggested that a reduction in the decelerative peak may signify an increased stride efficiency, by permitting a smoother transition from retardation to propulsion [78]. This may be important in determining the safety of racing surfaces also. However, although the impact accelerations were commonly lower when barefoot, it is worth noting that, when galloping barefoot on turf, a greater proportion of the runs involved the horses swapping leads (Supplementary Data File); 18% of mixed-lead fore-limb runs and 23% of mixed-lead hindlimb runs were from the barefoot–turf condition compared to just 7–9% of the data from the individual limbs. This could signify that the horses were more unbalanced in the barefoot–turf condition and may explain why the jockeys perceived gallop runs to be less smooth, most commonly variable and occasionally

unsafe (17% of trials) in this condition [71]. Hoof acceleration signals at different stages of the trimming/shoeing cycle will also be important to understand. For example, a gradual dorsal shift in the centre of pressure with respect to the distal interphalangeal joint due to hoof growth and backward tilting of the foot in unshod hooves [84] may influence the depth of penetration of the heel into a compliant surface during loading. Indeed, hoof pitch rotation during early stance if horses' heels sink into a surface has been reported at walk [90]. This effect may influence the magnitude of impact accelerations being recorded at the hoof wall.

4.2. Foot-Off

At foot-off, the large acceleration spikes are caused by the hoof accelerating to the forward speed of the horse. Accelerations were more similar between turf and artificial surfaces when compared to the impact data (Figure 3, Supplementary Table S4) but were almost always larger on the artificial surface. The maximum absolute differences occurred in the leading forelimb between surfaces for the z-maximum and y-maximum (difference of 12.6 g and 10.4 g, respectively), and this may reflect the fact that, in this limb, the braking and vertical impulses must decelerate the centre of mass and provide it with sufficient upward vertical velocity for the flight phase of the stride [81]. Vertical centre of mass displacements were indeed larger by around 5.7 mm downward and 2.5 mm upward on the artificial surface as a result of this action [70] (Figure A6; Figure A7). The general trend toward higher hoof accelerations on the artificial surface is also consistent with a faster breakover on this surface [26]. Larger acceleration peaks at foot-off have previously been related to faster track rebound rates and reduced hardness [78]. Here, the more deformable artificial track may return greater energy to the hoof during the propulsive phase, leading to a more energy-efficient gait and also explaining these higher accelerations. Nevertheless, even if an artificial surface might be deemed favourable, as the majority of UK racing currently takes place on turf tracks, there may be logistical constraints in the immediate future.

Consistent with the impact data, we found that the barefoot hoof had the lowest hoof accelerations on average across all stride times. Considering all acceleration axes together, our data indicate that foot-off accelerations were 4–7% higher in aluminium shoes, 5–6% higher in GluShus and 8–12% higher in steel shoes, when compared to the barefoot condition (comparisons made in the individual limbs). The pairwise comparisons with the largest offsets included barefoot in 18/36 cases; however, in two of these instances (for the x-minimum), the barefoot condition actually had the larger accelerations of the two shoeing conditions. In some ways, these observations are surprising because a barefoot hoof would be expected to deform more on impact and subsequently return more energy to the hoof, which might be expected to lead to more rapid accelerations. Indeed, at the higher gallop speeds, barefoot hooves do appear to experience proportionally higher foot-off accelerations relative to the shod conditions (Figure 4). This is consistent with observations that breakover becomes relatively faster for barefoot hooves at higher gallop speeds in the non-leading hindlimb; the only limb in which breakover duration was found to be sensitive to shoeing condition [26]. This previous work [26] also indicated that, at low gallop speeds, barefoot hooves have a longer breakover duration relative to the shod conditions (in the non-leading hindlimb). It was proposed that shoe shape, and in particular the bevelled toe of the shoes, might be important for increasing the breakover rate [26] and, by extrapolation here, hoof accelerations also, in the shod conditions at low–moderate speeds. As the retired ex-racehorses used in this study tended to gallop at average speeds of around 40 km h⁻¹, this may explain why accelerations associated with the barefoot condition tended to be reduced on average. In addition, given it was the mixed lead data that represented more of the faster barefoot runs (Supplementary Data File), it is consistent that an analysis of the barefoot condition in the individual limb datasets (for lower stride times) would tend toward lower values. Interestingly, it was the non-leading hindlimb that experienced slightly higher accelerations overall at foot-off compared to the other limbs (up to 6% higher

on average across all acceleration axes), and this may explain its sensitivity to shoeing conditions in terms of breakover duration [26].

At the upper range of gallop speeds assessed here, the foot-off accelerations were increased across all acceleration axes proportionally more in the hindlimbs compared to the forelimbs, with the exception of the x-minimum in the non-leading hindlimb. This trend also mirrors the observations in the breakover duration data [26]. It likely relates to a difference in landing orientation and subsequent hoof trajectory in forelimbs versus hindlimbs as speeds increase, including greater hindlimb loading and more rapid push-off from the hind end. Further work is needed to establish the effect of turns on hoof acceleration patterns, as turning imposes additional asymmetrical forces on the limbs on the inside and outside of the turn [91]. The effect of hoof growth on foot-off accelerations is also potentially important. Long toes may lead to longer breakover durations, and due to an increase in the length of the resistance arm, there will be an increase in tension on the deep digital flexor tendon to initiate breakover [92], and toe-penetration depth is likely to increase. Extending the duration of breakover could reduce the magnitude of accelerations in the foot-off window.

5. Conclusions

Tri-axial hoof accelerations at impact and foot-off in galloping Thoroughbreds were influenced by the horses' shoeing condition and surface type. Accelerations were elevated at impact on the turf surface compared to the artificial track by 1.2–2.4 times across limbs, depending on the acceleration axis considered; acceleration magnitudes were largest and offsets between surfaces greatest along the hoof wall and in the dorso-palmar direction. Accelerations were, on average, 2–18% higher at impact in the shod conditions compared to barefoot, when considering all acceleration axis directions together, but they rose up to 30% more in steel. Preventing excessive shock loading and related musculoskeletal injuries in racehorses is of critical relevance to the racing industry. This work suggests that the combination of an artificial surface and barefoot hooves may be beneficial for minimising the exposure of the hoof and distal limb to large accelerations during hoof landing. At foot-off, it was most commonly observed that accelerations were amplified on the artificial surface compared to the turf; average accelerations per individual limb were 2–12% greater for the former. We inferred that the artificial surface deformed, at least to some extent, more elastically under load and subsequently recovered and returned a higher proportion of energy to the hoof. This will have aided propulsion, leading to more rapid hoof breakover, and it could confer a performance benefit. Overall, barefoot hooves typically experienced the lowest accelerations at foot-off; however, at top gallop speeds, accelerations for barefoot hooves appeared to increase at a relatively higher rate than for shod conditions. Further work is needed to relate these findings to injury risk and racing outcomes specifically, particularly in racehorses galloping at top speeds.

Supplementary Materials: The following supporting information can be downloaded at <https://www.mdpi.com/article/10.3390/ani12172161/s1>. Supplementary Data File containing the following: Full raw data spreadsheet with data dictionary. Table S1: Significance values for the entire dataset and a subset of the data with stride frequencies of 2 Hz and above. Table S2: Estimated marginal means for shoeing condition effects (all data). Table S3: Post hoc pairwise comparisons (with Bonferroni correction) for shoeing conditions, using peak impact and foot-off accelerations. The entire dataset was used here (i.e., across all stride times). Table S4: Estimated marginal means for surface effects (all data). Table S5: Post hoc pairwise comparisons (with Bonferroni correction) for surfaces, using peak impact and foot-off accelerations. The entire dataset was used here (i.e., across all stride times). Table S6: Estimated marginal means for shoeing condition and surface effects (all data). Table S7: Post hoc pairwise comparisons (with Bonferroni correction) for shoe–surface combinations, using peak impact and foot-off accelerations. The entire dataset was used here (i.e., across all stride times). Table S8: Significance values for area values within 5 ms of the maximum acceleration (entire dataset). Table S9: Estimated marginal means for shoeing conditions, using area data. The entire dataset was used here (i.e., across all stride times). Table S10: Estimated marginal means for surface conditions,

using area data. The entire dataset was used here (i.e., across all stride times). Table S11: Estimated marginal means for shoe–surface conditions, using area data. The entire dataset was used here (i.e., across all stride times).

Author Contributions: Conceptualization, K.H. and T.P.; methodology, K.H., P.D., T.P. and M.P.; formal analysis, K.H.; investigation, K.H., J.C., K.K., P.D., H.C., L.B., D.H., L.H. and S.M.; data curation, K.H.; writing—original draft preparation, K.H.; writing—review and editing, K.H. and T.P.; visualization, K.H.; supervision, T.P.; project administration, K.H.; funding acquisition, T.P. All authors have read and agreed to the published version of the manuscript.

Funding: This research was funded by the Horserace Betting Levy Board project 4497, Prj786, grant titled “S.A.F.E.R.” (Shoe Assessment for Equine Racing).

Institutional Review Board Statement: An ethical review was performed and approval was granted for this study by the Royal Veterinary College Clinical Research Ethical Review Board (URN 2018 1841-2, 19 November 2018).

Data Availability Statement: Data supporting the results are presented in the Results section of this manuscript and the Supplementary Data File.

Acknowledgments: The authors would like to thank the British Racing School for facilitating access to horses, jockeys and facilities. Jessica Josephson, Edward Evans, Alice Morrell, Morgan Ruble and Hazel Birch-Ellis from the Royal Veterinary College and Simon Curtis are all thanked for their assistance and support with data collection.

Conflicts of Interest: We have the following interests: J.C. owns the company James Coburn AWCF Farriers Ltd., which employed D.H., L.B. and H.C. at the time of the study; J.C., P.D., H.C., D.H. and L.B. are now registered farriers; M.P. is the director of the Racetrack Safety Program and Principal of the company Biologically Applied Testing LLC; T.P. is the owner of Equigait, a provider of gait analysis products and services. This does not alter our adherence to all policies on sharing data and materials. The funders had no role in the design of the study; in the collection, analyses or interpretation of data; in the writing of the manuscript; or in the decision to publish the results.

Appendix A Supplementary Information

Appendix A.1 Peak Impact and Foot-Off Accelerations across All Acceleration Parameters

Appendix A Figures A1 and A2 illustrate the trends in peak accelerations across individual limbs for each of the six acceleration parameters, subdivided by the shoe–surface combination, at impact and foot-off, respectively.

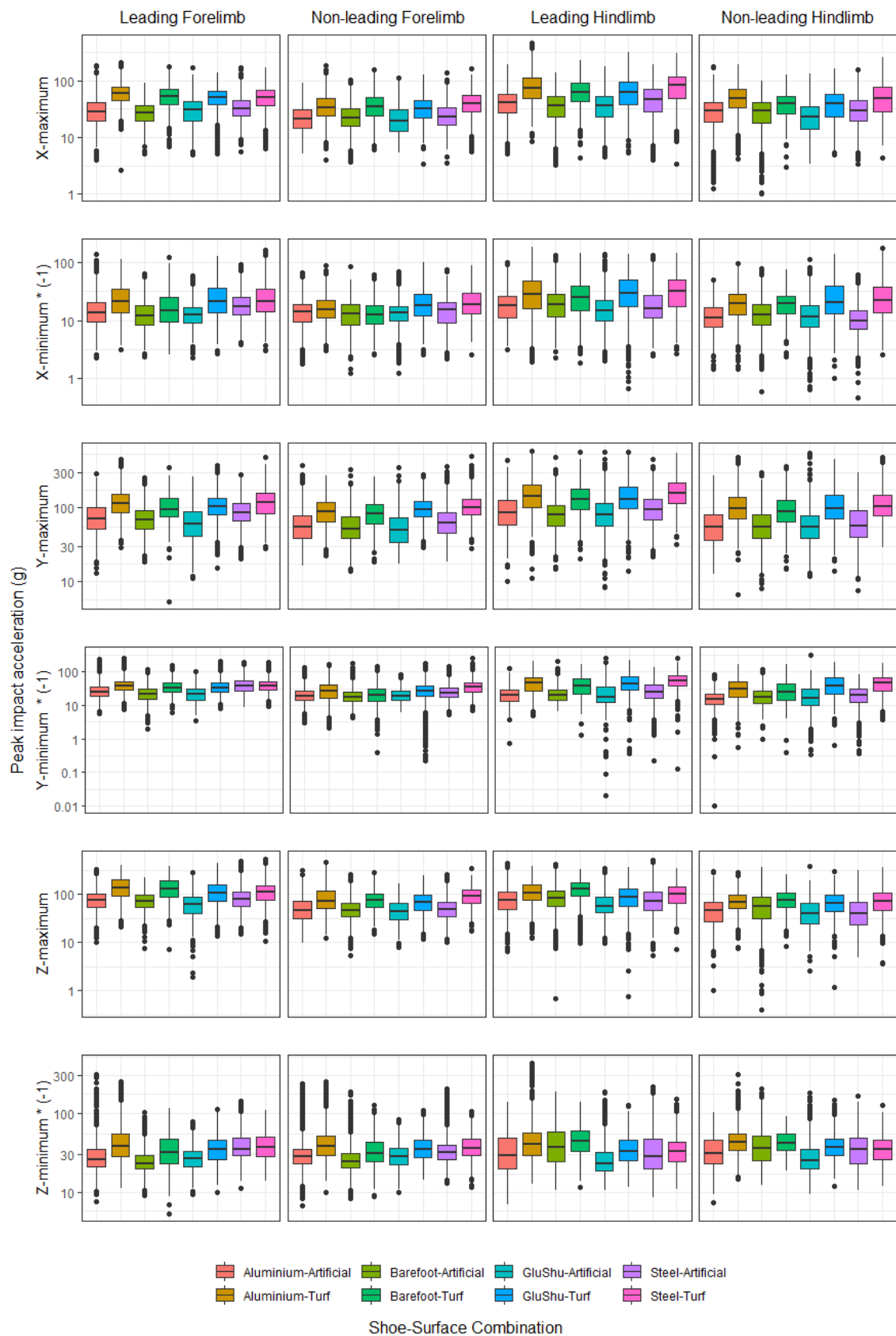


Figure A1. Boxplots illustrating minimum and maximum impact accelerations per shoe–surface combination. The *p*-values for pairwise comparisons (with Bonferroni correction) are provided in Supplementary Table S7. Please note that ‘*’ indicates ‘multiplied by’.

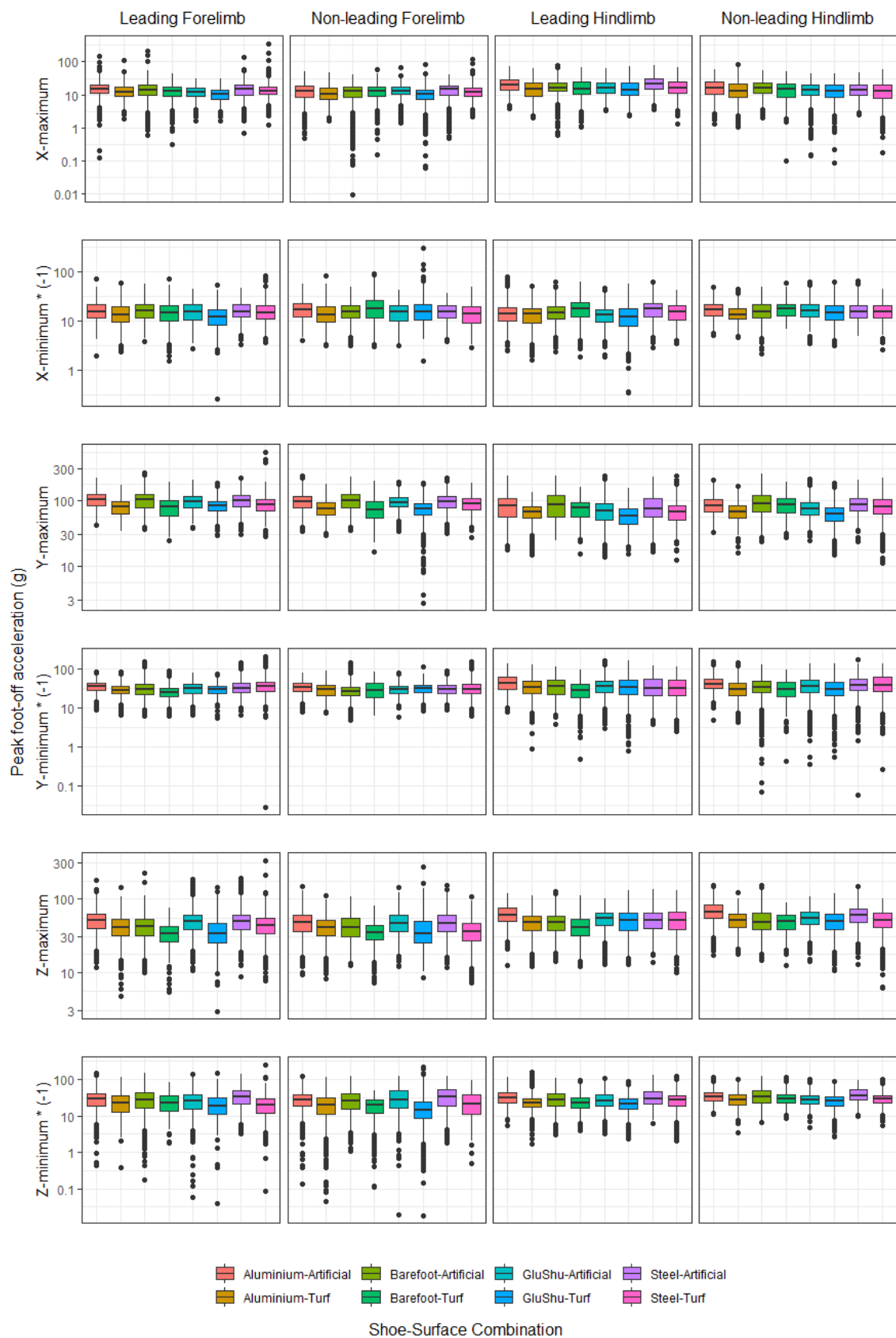


Figure A2. Boxplots illustrating minimum and maximum foot-off accelerations per shoe–surface combination. The *p*-values for pairwise comparisons (with Bonferroni correction) are provided in Supplementary Table S7. Please note that ‘*’ indicates ‘multiplied by’.

Appendix A.2 Peak Impact and Foot-Off Correlations

To assess which impact and foot-off parameters were most closely related, Pearson Product Moment Correlation Coefficients were calculated for comparisons between each of the impact and foot-off parameters and stride time. The results are presented in Appendix A Figure A3. The amplitudes of the minimum and maximum parameters were inversely correlated with stride time, with the strongest correlation occurring between stride time and y-maximum at foot-off (correlation coefficient = -0.67). X-maximum at impact was most strongly correlated with the y- and z-maximum accelerations at impact (correlation coefficients of 0.71 and 0.57 , respectively), but also showed a moderate correlation with the x-minimum at impact (correlation coefficient = -0.51). The x-minimum at impact was moderately correlated with the y-maximum at impact (correlation coefficient = -0.53). The impact y-maximum showed moderate correlations with the y-minimum and z-maximum at impact (correlation coefficients of -0.64 and 0.64 , respectively), whereas the impact y-minimum was weakly correlated with the impact z-maximum (-0.52). At foot-off, the y-maximum additionally showed a moderate correlation with both the y-minimum and the z-minimum (correlation coefficients of -0.54 and -0.57 , respectively). All other correlation coefficients were ≤ 0.5 .

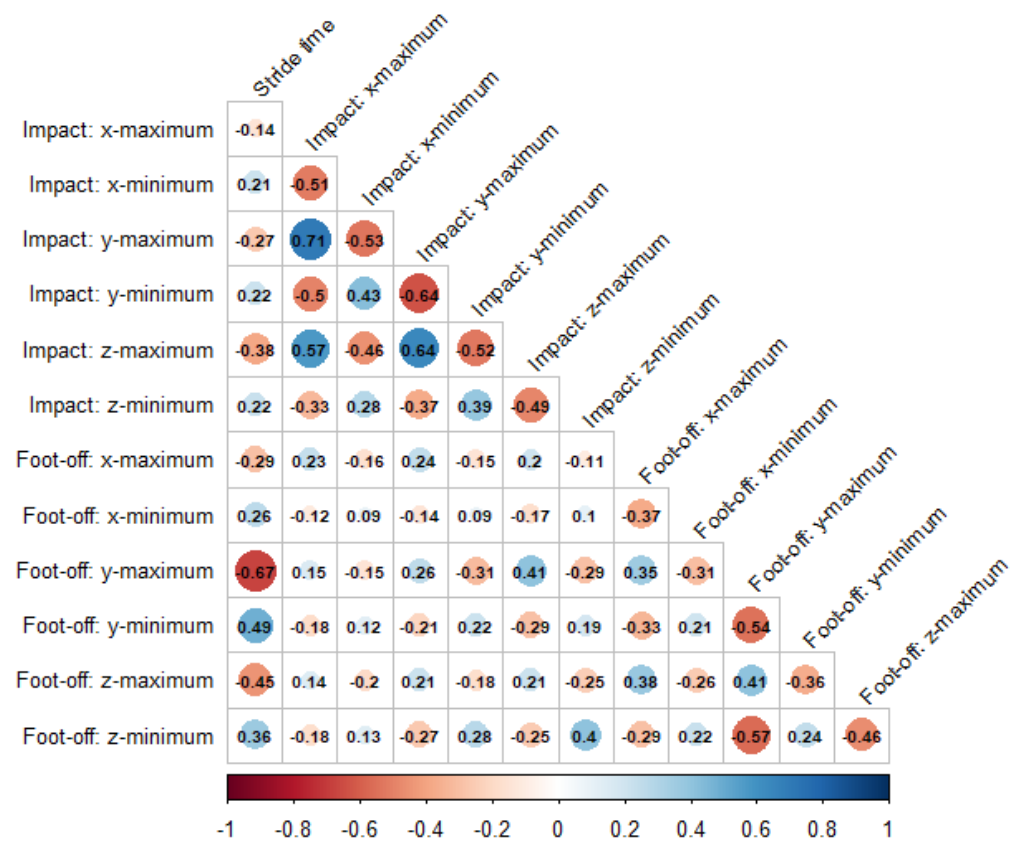


Figure A3. Correlation matrix outlining the Pearson Product Moment Correlation Coefficient amongst minimum and maximum acceleration parameters. All data are included here from all limbs.

Appendix A.3 Relationship between Stride Time and Impact and Foot-Off Correlations

Appendix A Figure A4 illustrates the trends between stride time and the accelerations at impact and foot-off for each of the individual limbs.

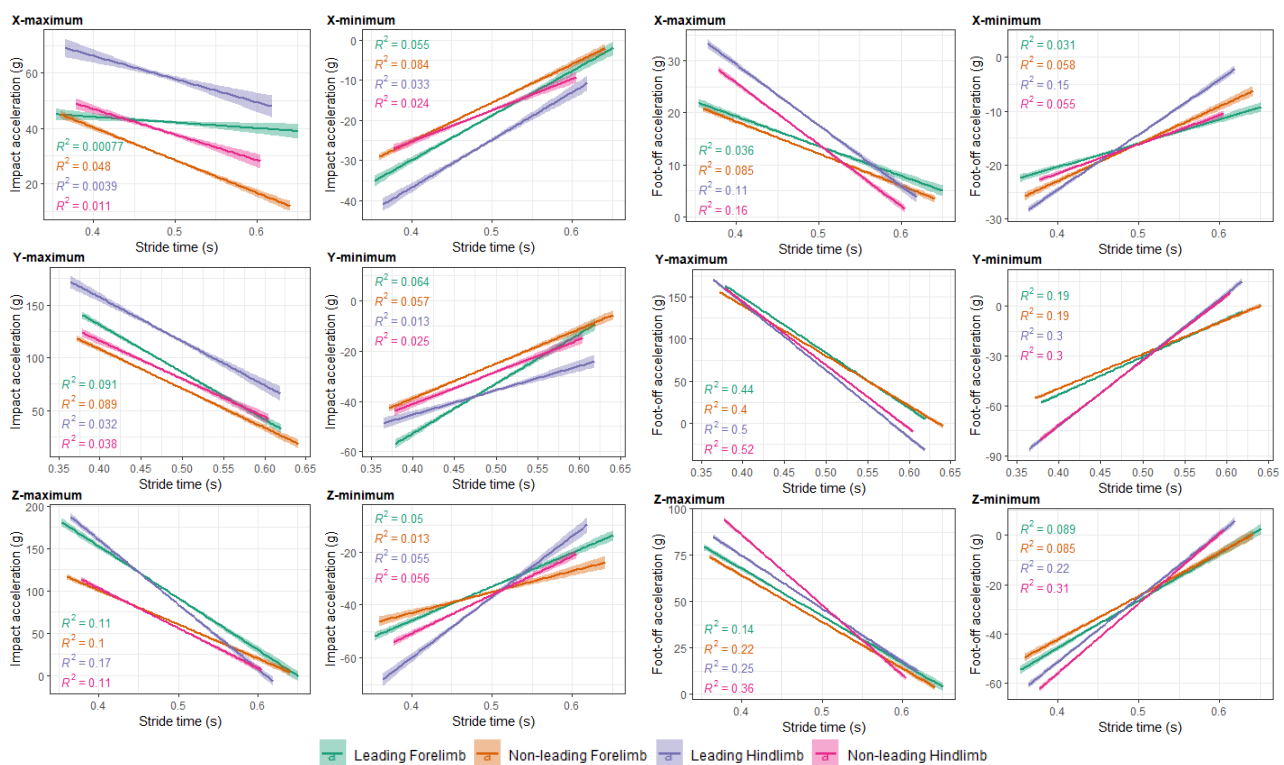


Figure A4. Relationship between stride time and the impact and foot-off accelerations. Data are subdivided according to acceleration parameter for each limb. The r^2 and p values for the linear regressions are indicated on the subplots. The shaded areas represent the 95% confidence intervals for predictions from a linear model. All $p < 0.001$.

Appendix A.4 Peak Accelerations versus Areas

We considered trends in area data to be more meaningful than absolute values because we arbitrarily selected a given timeframe away from minimum and maximum peaks to study. The justification for the time window chosen was provided in Section 3.1. Appendix A Figure A5 illustrates the trends amongst shoe–surface conditions for the summed (positive) acceleration data in the 5 ms window ahead of the maximum for comparison to the plots in Appendix A Figures A1 and A2. For the impact phase, the area data indicated that accelerations were larger for the leading compared to the non-leading limbs, and it was clearly apparent that the areas for the turf were larger than those for the artificial surface. The inter-quartile ranges for the turf data were also typically larger than for the artificial surface. Shoe effects were subtler, but when looking at the y-maximum parameter (the focus of Section 3.6 also), the steel–turf condition once again had the largest accelerations. At foot-off, accelerations were larger on the artificial surface compared to the turf, with the exception of the x-axis data in the forelimbs (Table S10).

Therefore, the area results appeared to largely mimic those of the peak impact and foot-off accelerations. To investigate this relationship in more detail, the area data were plotted against the peak acceleration data, and the relationships were modelled by a linear regression for each limb (Appendix A Figure A6). There was a significant positive correlation between peak values and area data in all cases, but the correlation was most strong for the area versus y-maximum peak acceleration datasets at foot-off (mean $r^2 = 0.76$).

Please note that all the raw area data are available in the Supplementary Data File. Linear mixed models were run on the summed (positive) acceleration data in the 5 ms window ahead of the maximum and the significance values, and the estimated marginal mean outputs from these statistical analyses are provided in the Supplementary Tables S8–S11).

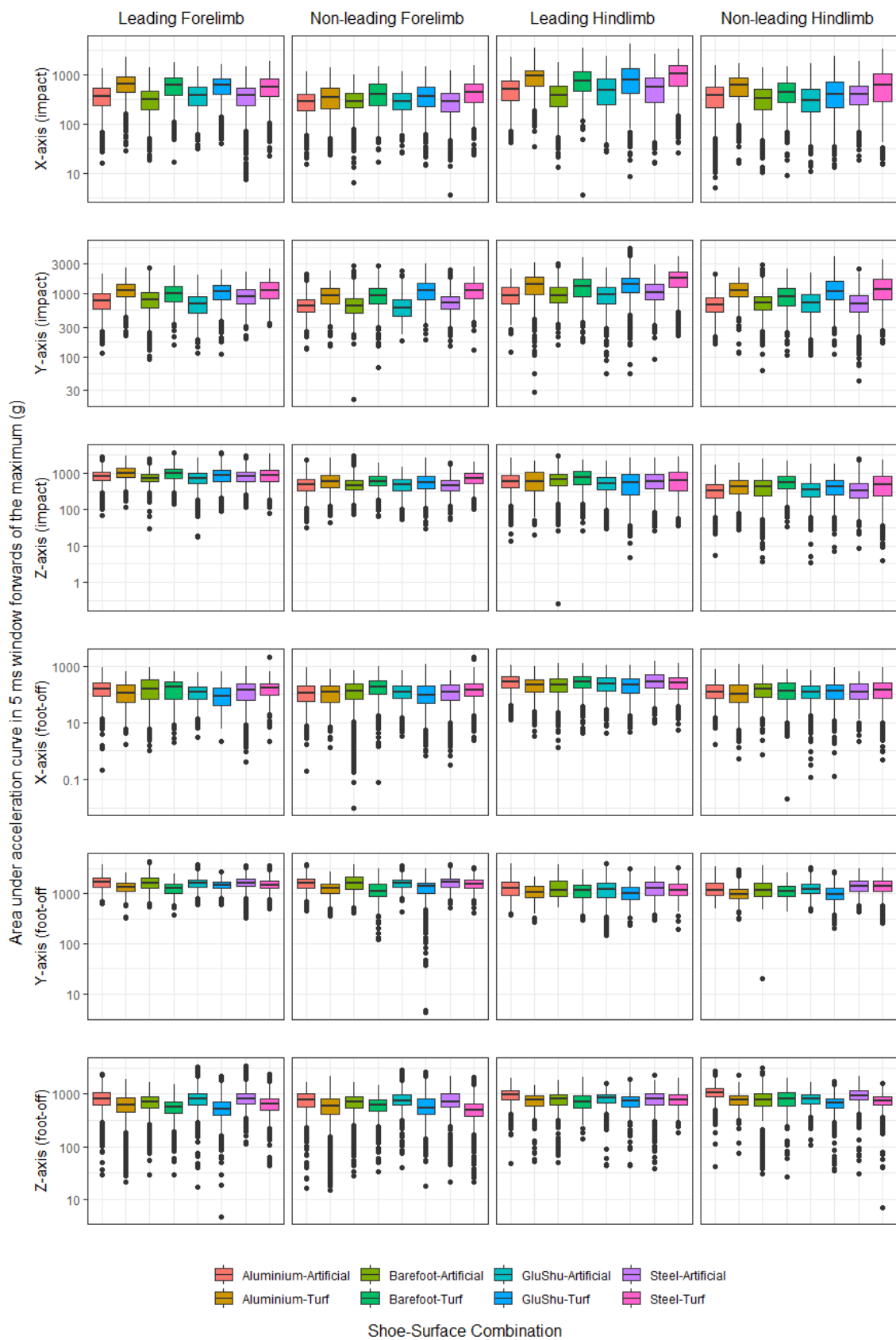


Figure A5. Boxplots illustrating the summed (positive) acceleration data in the 5 ms window ahead of the maximum, subdivided according to shoe–surface condition.

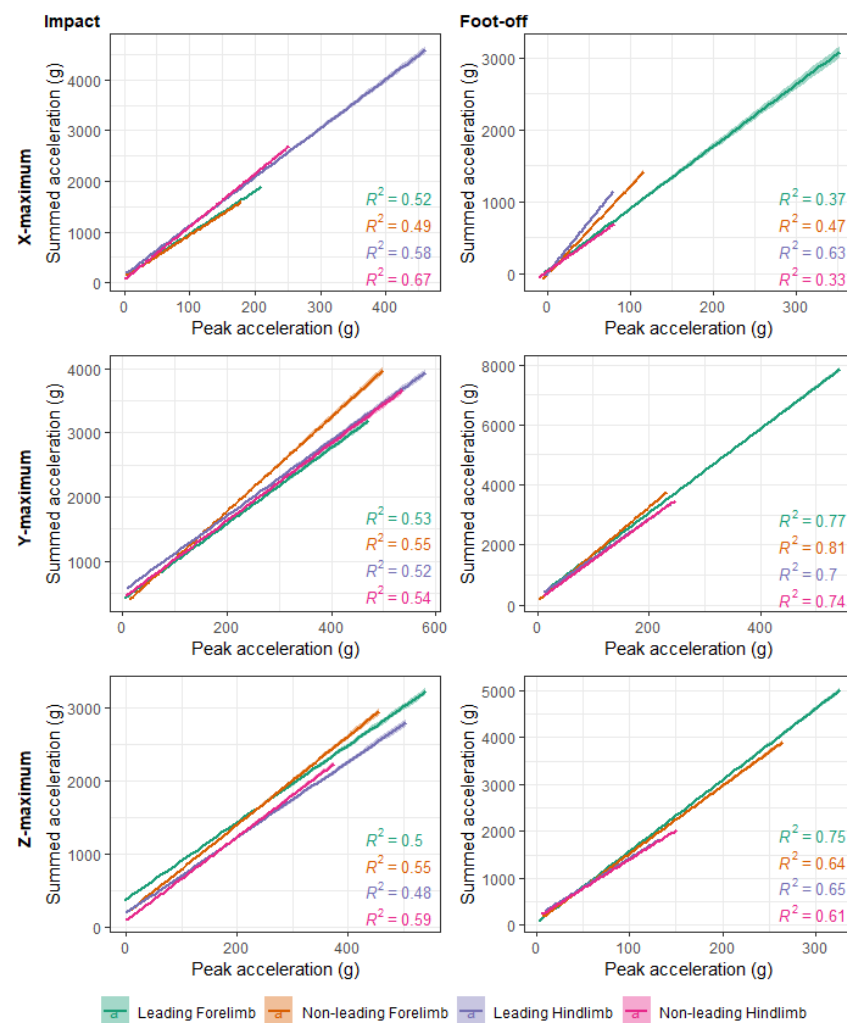


Figure A6. Positive linear relationships between peak accelerations and summed accelerations (positive) within 5 ms forward in time of the maximum peak. Data are subdivided according to acceleration parameter for each limb. All $p < 0.001$.

Appendix A.5 Relationship between Hoof Accelerometry Data and Centre of Mass Displacements

Scatter plots were used to investigate whether the hoof acceleration patterns were correlated with the tri-axial centre of mass displacements of the horses reported previously [70], and these are presented in Appendix A Figures A7 and A8. In summary, weak-to-moderate correlations were found between the tri-axial hoof impact acceleration parameters and the tri-axial centre of mass displacements (Figure A7). The dorso-ventral centre-of-mass minimum values were most closely related to the hoof data, with correlation coefficients of $r^2 = 0.76$ and $r^2 = 0.72$ for the y-minimum and y-maximum parameters, respectively. The foot-off accelerations were not closely correlated with the centre of mass data (Appendix A Figure A8).

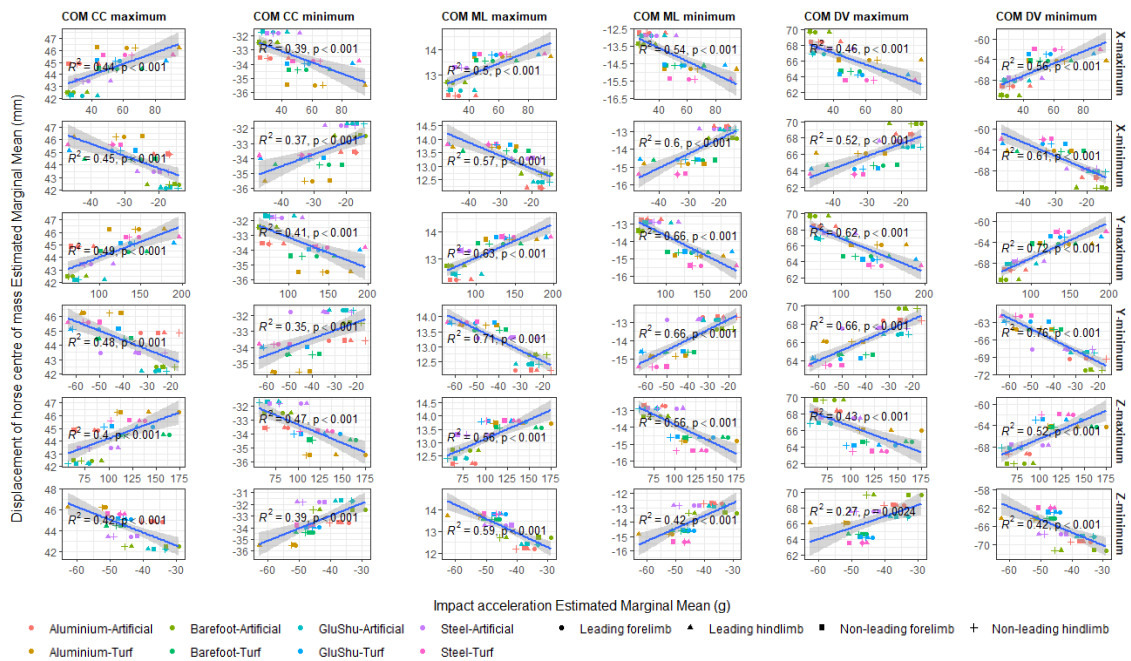


Figure A7. Relationship between impact acceleration data and centre of mass (COM) displacements. Data are subdivided horizontally by the hoof acceleration parameters (x-maximum, x-minimum, y-maximum, y-minimum, z-maximum and z-minimum) and vertically by the COM parameters (CC-maximum, CC-minimum, ML-maximum, ML-minimum, DV-maximum and DV-minimum), as indicated by the labels on the right and top sides of this figure. Within each subplot, the data are further subdivided according to both shoe–surface combination and limb.

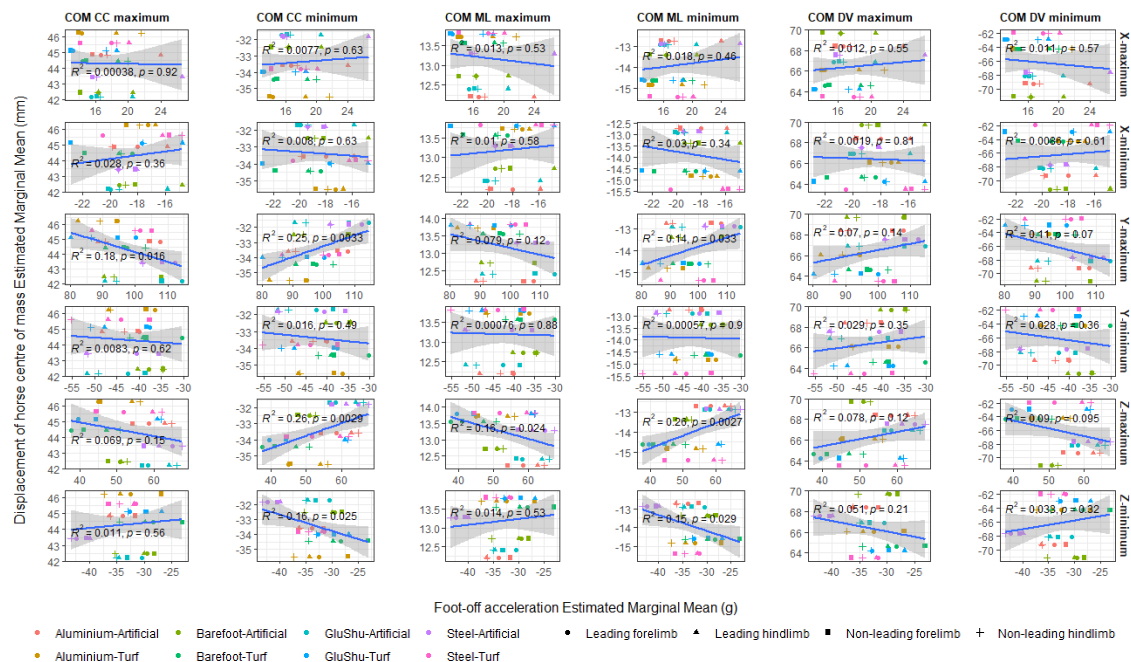


Figure A8. Relationship between foot-off acceleration data and centre of mass (COM) displacements. Data are subdivided horizontally by the hoof acceleration parameters (x-maximum, x-minimum, y-maximum, y-minimum, z-maximum and z-minimum) and vertically by the COM parameters (CC-maximum, CC-minimum, ML-maximum, ML-minimum, DV-maximum and DV-minimum), as indicated by the labels on the right and top sides of this figure. Within each subplot, the data are further subdivided according to both shoe–surface combination and limb.

References

1. Hitchens, P.L.; Morrice-West, A.V.; Stevenson, M.A.; Whitton, R.C. Meta-analysis of risk factors for racehorse catastrophic musculoskeletal injury in flat racing. *Vet. J.* **2019**, *245*, 29–40. [[CrossRef](#)] [[PubMed](#)]
2. Williams, R.B.; Harkins, L.S.; Hammond, C.J.; Wood, J.L.N. Racehorse injuries, clinical problems and fatalities recorded on British racecourses from flat racing and National Hunt racing during 1996, 1997 and 1998. *Equine Vet. J.* **2001**, *33*, 478–486. [[CrossRef](#)] [[PubMed](#)]
3. Parkin, T.D.H. Epidemiology of Racetrack Injuries in Racehorses. *Vet. Clin. North Am. Equine Pract.* **2008**, *24*, 1–19. [[CrossRef](#)] [[PubMed](#)]
4. Cogger, N.; Perkins, N.; Hodgson, D.R.; Reid, S.W.J.; Evans, D.L. Risk factors for musculoskeletal injuries in 2-year-old Thoroughbred racehorses. *Prev. Vet. Med.* **2006**, *74*, 36–43. [[CrossRef](#)]
5. Ely, E.R.; Avella, C.S.; Price, J.S.; Smith, R.K.W.; Wood, J.L.N.; Verheyen, K.L.P. Descriptive epidemiology of fracture, tendon and suspensory ligament injuries in National Hunt racehorses in training. *Equine Vet. J.* **2009**, *41*, 372–378. [[CrossRef](#)]
6. Self Davies, Z.T.; Spence, A.J.; Wilson, A.M. Ground reaction forces of overground galloping in ridden Thoroughbred racehorses. *J. Exp. Biol.* **2019**, *222*, jeb204107. [[CrossRef](#)]
7. Witte, T.H.; Knill, K.; Wilson, A.M. Determination of peak vertical ground reaction force from duty factor in the horse (*Equus caballus*). *J. Exp. Biol.* **2004**, *207*, 3639–3648. [[CrossRef](#)]
8. Thomason, J.J.; Peterson, M.L. Biomechanical and Mechanical Investigations of the Hoof-Track Interface in Racing Horses. *Vet. Clin. North Am.-Equine Pract.* **2008**, *24*, 57–77. [[CrossRef](#)]
9. Wilson, A.M.; McGuigan, M.P.; Su, A. Horses damp the spring in their step. *Nature* **2001**, *414*, 895–899. [[CrossRef](#)]
10. Gustas, P.; Johnston, C. In vivo transmission of impact shock waves in the distal forelimb of the horse. *Equine Vet. J.* **2001**, *33*, 11–15. [[CrossRef](#)]
11. Willemen, M.A.; Jacobs, M.W.H.; Schamhardt, H.C. In vitro transmission and attenuation of impact vibrations in the distal forelimb. *Equine Exerc. Physiol.* **1999**, *30*, 245–248. [[CrossRef](#)] [[PubMed](#)]
12. Benoit, P.; Barrey, E.; Regnault, J.C.; Brochet, J.L. Comparison of the damping effect of different shoeing by the measurement of hoof acceleration. *Acta Anat.* **1993**, *146*, 109–113. [[CrossRef](#)]
13. Barrey, E.; Landjerit, B.; Wolter, R. Shock and vibration during the hoof impact on different track surfaces. *Equine Exerc. Physiol.* **1991**, *1*, 97–106.
14. Burn, J.F.; Wilson, A.; Nason, G.P. Impact during equine locomotion: Techniques for measurement and analysis. *Equine Vet. J. Suppl.* **1997**, *23*, 9–12. [[CrossRef](#)] [[PubMed](#)]
15. Burn, J.F. Time domain characteristics of hoof-ground interaction at the onset of stance phase. *Equine Vet. J.* **2006**, *38*, 657–663. [[CrossRef](#)] [[PubMed](#)]
16. Setterbo, J.J.; Garcia, T.C.; Campbell, I.P.; Reese, J.L.; Morgan, J.M.; Kim, S.Y.; Hubbard, M.; Stover, S.M. Hoof accelerations and ground reaction forces of Thoroughbred racehorses measured on dirt, synthetic, and turf track surfaces. *Am. J. Vet. Res.* **2009**, *70*, 1220–1229. [[CrossRef](#)]
17. Chateau, H.; Robin, D.; Falala, S.; Pourcelot, P.; Valette, J.P.; Ravary, B.; Denoix, J.M.; Crevier-Denoix, N. Effects of a synthetic all-weather waxed track versus a crushed sand track on 3D acceleration of the front hoof in three horses trotting at high speed. *Equine Vet. J.* **2009**, *41*, 247–251. [[CrossRef](#)]
18. Ryan, C.T.; Dallap Schaer, B.L.; Nunamaker, D.M. A novel wireless data acquisition system for the measurement of hoof accelerations in the exercising horse. *Equine Vet. J.* **2006**, *38*, 671–674. [[CrossRef](#)]
19. Pratt, G.W. Model for injury to the foreleg of the Thoroughbred racehorse. *Equine Vet. J.* **1997**, *29*, 30–32. [[CrossRef](#)]
20. Orlande, O.; Hobbs, S.J.; Martin, J.H.; Owen, A.G.; Northrop, A.J. Measuring hoof slip of the leading limb on jump landing over two different equine arena surfaces. *Comp. Exerc. Physiol.* **2012**, *8*, 33–39. [[CrossRef](#)]
21. Gustås, P.; Johnston, C.; Drevemo, S. Ground reaction force and hoof deceleration patterns on two different surfaces at the trot. *Equine Comp. Exerc. Physiol.* **2006**, *3*, 209–216. [[CrossRef](#)]
22. Ruina, A.; Bertram, J.E.A.; Srinivasan, M. A collisional model of the energetic cost of support work qualitatively explains leg sequencing in walking and galloping, pseudo-elastic leg behavior in running and the walk-to-run transition. *J. Theor. Biol.* **2005**, *237*, 170–192. [[CrossRef](#)] [[PubMed](#)]
23. Hobbs, S.J.; Clayton, H.M. Sagittal plane ground reaction forces, centre of pressure and centre of mass in trotting horses. *Vet. J.* **2013**, *198*, 14–19. [[CrossRef](#)] [[PubMed](#)]
24. Johnston, C.; Back, W. Hoof ground interaction: When biomechanical stimuli challenge the tissues of the distal limb. *Equine Vet. J.* **2006**, *38*, 634–641. [[CrossRef](#)] [[PubMed](#)]
25. Reiser-II, R.F.; Peterson, M.L.; McIlwraith, C.W.; Woodward, B. Simulated effects of racetrack material properties on the vertical loading of the equine forelimb. *Sports Eng.* **2000**, *3*, 1–11. [[CrossRef](#)]
26. Horan, K.; Coburn, J.; Kourdache, K.; Day, P.; Harborne, D.; Brinkley, L.; Carnall, H.; Hammond, L.; Peterson, M.; Millard, S.; et al. Influence of speed, ground surface and shoeing Condition on hoof breakover duration in galloping Thoroughbred racehorses. *Animals* **2021**, *11*, 2588.
27. Radin, E.L. Subchondral bone changes and cartilage damage. *Equine Vet. J.* **1999**, *31*, 94–95. [[CrossRef](#)]
28. Whitton, R.C.; Ayodele, B.A.; Hitchens, P.L.; Mackie, E.J. Subchondral bone microdamage accumulation in distal metacarpus of Thoroughbred racehorses. *Equine Vet. J.* **2018**, *50*, 766–773. [[CrossRef](#)]

29. Firth, E.C.; Delahunt, J.; Wichtel, J.W.; Birch, H.L.; Goodship, A.E. Galloping exercise induces regional changes in bone density within the third and radial carpal bones of Thoroughbred horses. *Equine Vet. J.* **1999**, *31*, 111–115. [[CrossRef](#)]
30. Cheney, J.A.; Liou, S.Y.; Wheat, J.D. Cannon-bone fracture in the thoroughbred racehorse. *Med. Biol. Eng.* **1973**, *11*, 613–620. [[CrossRef](#)]
31. Drevemo, S.; Hjerten, G.; Johnston, C. Drop hammer tests of Scandinavian harness racetracks. *Equine Vet. J.* **1994**, *26*, 35–38. [[CrossRef](#)]
32. Crevier-Denoix, N.; Pourcelot, P.; Ravary, B.; Robin, D.; Falala, S.; Uzel, S.; Grison, A.C.; Valette, J.P.; Denoix, J.M.; Chateau, H. Influence of track surface on the equine superficial digital flexor tendon loading in two horses at high speed trot. *Equine Vet. J.* **2009**, *41*, 257–261. [[CrossRef](#)] [[PubMed](#)]
33. Crevier-Denoix, N.; Ravary-Plumioën, B.; Vergari, C.; Camus, M.; Holden-Douilly, L.; Falala, S.; Jerbi, H.; Desquilbet, L.; Chateau, H.; Denoix, J.M.; et al. Comparison of superficial digital flexor tendon loading on asphalt and sand in horses at the walk and trot. *Vet. J.* **2013**, *198*, e130–e136. [[CrossRef](#)] [[PubMed](#)]
34. Radin, E.L.; Orr, R.B.; Kelman, J.L.; Paul, I.L.; Rose, R.M. Effect of prolonged walking on concrete on the knees of sheep. *J. Biomech.* **1982**, *15*, 487–492. [[CrossRef](#)] [[PubMed](#)]
35. Simon, S.R.; Radin, E.L.; Paul, I.L.; Rose, R.M. The response of joints to impact loading. II. In vivo behavior of subchondral bone. *J. Biomech.* **1972**, *5*, 267–272. [[CrossRef](#)]
36. Hernandez, J.; Hawkins, D.L.; Scollay, M.C. Race-start characteristics and risk of catastrophic musculoskeletal injury in Thoroughbred racehorses. *J. Am. Vet. Med. Assoc.* **2001**, *218*, 83–86. [[CrossRef](#)]
37. Peterson, M.; Sanderson, W.; Kussainov, N.; Hobbs, S.J.; Miles, P.; Scollay, M.C.; Clayton, H.M. Effects of racing surface and turn radius on fatal limb fractures in thoroughbred racehorses. *Sustainability* **2021**, *13*, 539. [[CrossRef](#)]
38. Northrop, A.J.; Martin, J.H.; Holt, D.; Hobbs, S.J. Operational temperatures of all-weather thoroughbred racetracks influence surface functional properties. *Biosyst. Eng.* **2020**, *193*, 37–45. [[CrossRef](#)]
39. Peterson, M.L.; Reiser, R.F.; Kuo, P.H.; Radford, D.W.; McIlwraith, C.W. Effect of temperature on race times on a synthetic surface. *Equine Vet. J.* **2010**, *42*, 351–357. [[CrossRef](#)]
40. Mahaffey, C.A.; Peterson, M.L.; Roepstorff, L. The effects of varying cushion depth on dynamic loading in shallow sand thoroughbred horse dirt racetracks. *Biosyst. Eng.* **2013**, *114*, 178–186. [[CrossRef](#)]
41. Oikawa, M.; Kusunose, R. Fractures sustained by racehorses in Japan during flat racing with special reference to track condition and racing time. *Vet. J.* **2005**, *170*, 369–374. [[CrossRef](#)] [[PubMed](#)]
42. Bolwell, C.; Rogers, C.; Gee, E.; McIlwraith, W. Epidemiology of musculoskeletal injury during racing on New Zealand racetracks 2005–2011. *Animals* **2017**, *7*, 62. [[CrossRef](#)]
43. Rosanowski, S.M.; Chang, Y.M.; Stirk, A.J.; Verheyen, K.L.P. Descriptive epidemiology of veterinary events in flat racing Thoroughbreds in Great Britain (2000 to 2013). *Equine Vet. J.* **2017**, *49*, 275–281. [[CrossRef](#)] [[PubMed](#)]
44. Bailey, C.J.; Reidt, S.W.J.; Hodgson, D.R.; Bourke, J.M.; Rose, R.J. Flat, hurdle and steeple racing: Risk factors for musculoskeletal injury. *Equine Vet. J.* **1998**, *30*, 498–503. [[CrossRef](#)]
45. Henley, W.E.; Rogers, K.; Harkins, L.; Wood, J.L.N. A comparison of survival models for assessing risk of racehorse fatality. *Prev. Vet. Med.* **2006**, *74*, 3–20. [[CrossRef](#)] [[PubMed](#)]
46. Boden, L.A.; Anderson, G.A.; Charles, J.A.; Morgan, K.L.; Morton, J.M.; Parkin, T.D.H.; Clarke, A.F.; Slocombe, R.F. Risk factors for Thoroughbred racehorse fatality in flat starts in Victoria, Australia (1989–2004). *Equine Vet. J.* **2007**, *39*, 430–437. [[CrossRef](#)] [[PubMed](#)]
47. Parkin, T.D.H.; Clegg, P.D.; French, N.P.; Proudman, C.J.; Riggs, C.M.; Singer, E.R.; Webbon, P.M.; Morgan, K.L. Risk of fatal distal limb fractures among Thoroughbreds involved in the five types of racing in the United Kingdom. *Vet. Rec.* **2004**, *154*, 493–497. [[CrossRef](#)]
48. Reardon, R.J.M.; Boden, L.; Stirk, A.J.; Parkin, T.D.H. Accuracy of distal limb fracture diagnosis at British racecourses 1999–2005. *Vet. Rec.* **2014**, *174*, 477. [[CrossRef](#)]
49. Parkin, T.D.H.; Clegg, P.D.; French, N.P.; Proudman, C.J.; Riggs, C.M.; Singer, E.R.; Webbon, P.M.; Morgan, K.L. General Articles Risk factors for fatal lateral condylar fracture of the third metacarpus/metatarsus in UK racing. *Equine Vet. J.* **2004**, *37*, 192–199. [[CrossRef](#)]
50. Georgopoulos, S.P.; Parkin, T.D.H. Risk factors for equine fractures in Thoroughbred flat racing in North America. *Prev. Vet. Med.* **2017**, *139*, 99–104. [[CrossRef](#)]
51. Kristoffersen, M.; Parkin, T.D.H.; Singer, E.R. Catastrophic biaxial proximal sesamoid bone fractures in UK Thoroughbred races (1999–2004): Horse characteristics and racing history. *Equine Vet. J.* **2010**, *42*, 420–424. [[CrossRef](#)] [[PubMed](#)]
52. Parkin, T.D.H.; Clegg, P.D.; French, N.P.; Proudman, C.J.; Riggs, C.M.; Singer, E.R.; Webbon, P.M.; Morgan, K.L. Catastrophic fracture of the lateral condyle of the third descriptions and pre-existing pathology. *Vet. J.* **2006**, *171*, 157–165. [[CrossRef](#)] [[PubMed](#)]
53. Kane, A.J.; Stover, S.M.; Gardner, I.A.; Case, J.T.; Johnson, B.J.; Read, D.H.; Ardans, A.A. Horseshoe characteristics as possible risk factors for fatal musculoskeletal injury of Thoroughbred racehorses. *Am. J. Vet. Res.* **1996**, *57*, 1147–1152.
54. Hill, A.E.; Gardner, I.A.; Carpenter, T.E.; Stover, S.M. Effects of injury to the suspensory apparatus, exercise, and horseshoe characteristics on the risk of lateral condylar fracture and suspensory apparatus failure in forelimbs of Thoroughbred racehorses. *Am. J. Vet. Res.* **2004**, *65*, 1508–1517. [[CrossRef](#)] [[PubMed](#)]

55. Hernandez, J.A.; Scollay, M.C.; Hawkins, D.L.; Corda, J.A.; Krueger, T.M. Evaluation of horseshoe characteristics and high-speed exercise history as possible risk factors for catastrophic musculoskeletal injury in Thoroughbred racehorses. *Am. J. Vet. Res.* **2005**, *66*, 1314–1320. [[CrossRef](#)] [[PubMed](#)]
56. Peel, J.A.; Peel, M.B.; Davies, H.M.S. The effect of gallop training on hoof angle in Thoroughbred racehorses. *Equine Vet. J.* **2006**, *38*, 431–434. [[CrossRef](#)]
57. Dabareiner, R.M.; Carter, G.K. Diagnosis, treatment, and farriery for horses with chronic heel pain. *Vet. Clin. North Am.-Equine Pract.* **2003**, *19*, 417–441. [[CrossRef](#)]
58. Kane, A.J.; Stover, S.M.; Gardner, I.A.; Bock, K.B.; Case, J.T.; Johnson, B.J.; Anderson, M.L.; Barr, B.C.; Daft, B.M.; Kinde, H.; et al. Hoof size, shape, and balance as possible risk factors for catastrophic musculoskeletal injury of Thoroughbred racehorses. *Am. J. Vet. Res.* **1998**, *59*, 1545–1552.
59. Anderson, T.M.; McIlwraith, C.W.; Douay, P. The role of conformation in musculoskeletal problems in the racing Thoroughbred. *Equine Vet. J.* **2004**, *36*, 571–575. [[CrossRef](#)]
60. Holroyd, K.; Dixon, J.J.; Mair, T.; Bolas, N.; Bolt, D.M.; David, F.; Weller, R. Variation in foot conformation in lame horses with different foot lesions. *Vet. J.* **2013**, *195*, 361–365. [[CrossRef](#)]
61. Eliashar, E.; McGuigan, M.P.; Wilson, A.M. Relationship of foot conformation and force applied to the navicular bone of sound horses at the trot. *Equine Vet. J.* **2004**, *36*, 431–435. [[CrossRef](#)] [[PubMed](#)]
62. Day, P.; Butts, D.; Pfau, T.; Pardoe, C.; Weller, R. Does hoof deformation differ between horses with collapsed heels and horses with non-collapsed heels? *J. Equine Vet. Sci.* **2013**, *10*, 859. [[CrossRef](#)]
63. Yoshihara, E.; Takahashi, T.; Otsuka, N.; Isayama, T.; Tomiyama, T.; Hiraga, A.; Wada, S. Heel movement in horses: Comparison between glued and nailed horse shoes at different speeds. *Equine Vet. J.* **2010**, *42*, 431–435. [[CrossRef](#)] [[PubMed](#)]
64. Mahaffey, C.A.; Peterson, M.L.; Thomason, J.J.; McIlwraith, C.W. Dynamic testing of horseshoe designs at impact on synthetic and dirt Thoroughbred racetrack materials. *Equine Vet. J.* **2016**, *48*, 97–102. [[CrossRef](#)] [[PubMed](#)]
65. Pardoe, C.H.; Mcguigan, M.P.; Rogerst, K.M.; Rowet, L.L.; Wilson, A.M.; Basic, V.; Royal, T.; Colledge, V.; Mymms, N. The effect of shoe material on the kinetics and kinematics of foot slip at impact on concrete. *Equine Vet. J.* **2001**, *33*, 70–73. [[CrossRef](#)] [[PubMed](#)]
66. Balch, O.K.; Clayton, H.M.; Lanovaz, J.L. Weight- and length- induced changes in limb kinematics in trotting horses. *Proc. Am. Assoc. Equine Pract.* **1996**, *42*, 218–219.
67. Willemen, M.A.; Savelberg, H.H.C.M.; Barneveld, A. The improvement of the gait quality of sound trotting warmblood horses by normal shoeing and its effect on the load on the lower forelimb. *Livest. Prod. Sci.* **1997**, *52*, 145–153. [[CrossRef](#)]
68. Day, P.; Collins, L.; Horan, K.; Weller, R.; Pfau, T. The Effect of Tungsten Road Nails on Upper Body Movement Asymmetry in Horses Trotting on Tarmac. *J. Equine Vet. Sci.* **2020**, *90*, 1–5. [[CrossRef](#)]
69. British Horseracing Authority. British Horseracing Authority Rules of Racing 2 May 2022, version 2022.2. p. 69. Available online: <https://rules.britishhorseracing.com/#!/book/34> (accessed on 20 August 2022).
70. Horan, K.; Kourdache, K.; Coburn, J.; Day, P.; Carnall, H.; Harborne, D.; Brinkley, L.; Hammond, L.; Millard, S.; Lancaster, B.; et al. The effect of horseshoes and surfaces on horse and jockey centre of mass displacements at gallop. *PLoS ONE* **2021**, *16*, e0257820. [[CrossRef](#)]
71. Horan, K.; Kourdache, K.; Coburn, J.; Day, P.; Brinkley, L.; Carnall, H.; Harborne, D.; Hammond, L.; Millard, S.; Pfau, T. Jockey Perception of Shoe and Surface Effects on Hoof-Ground Interactions and Implications for Safety in the Galloping Thoroughbred Racehorse. *J. Equine Vet. Sci.* **2021**, *97*, 103327. [[CrossRef](#)]
72. Witte, T.H.; Hirst, C.V.; Wilson, A.M. Effect of speed on stride parameters in racehorses at gallop in field conditions. *J. Exp. Biol.* **2006**, *209*, 4389–4397. [[CrossRef](#)] [[PubMed](#)]
73. Barrey, E.; Evans, S.E.; Evans, D.L.; Curtis, R.A.; Quinton, R.; Rose, R.J. Locomotion evaluation for racing in thoroughbreds. *Equine Vet. J.* **2001**, *33*, 99–103. [[CrossRef](#)] [[PubMed](#)]
74. Robilliard, J.J.; Pfau, T.; Wilson, A.M. Gait characterisation and classification in horses. *J. Exp. Biol.* **2007**, *210*, 187–197. [[CrossRef](#)] [[PubMed](#)]
75. Johnson, J.L.; Moore-Colyer, M. The relationship between range of motion of lumbosacral flexion-extension and canter velocity of horses on a treadmill. *Equine Vet. J.* **2009**, *41*, 301–303. [[CrossRef](#)] [[PubMed](#)]
76. Barstow, A. Does ‘hacking’ surface type affect equine forelimb foot placement, movement symmetry or hoof impact deceleration during ridden walk and trot exercise? *Equine Vet. J.* **2019**, *51*, 108–114. [[CrossRef](#)]
77. Chateau, H.; Holden, L.; Robin, D.; Falala, S.; Pourcelot, P.; Estoup, P.; Denoix, J.M.; Crevier-Denoix, N. Biomechanical analysis of hoof landing and stride parameters in harness trotter horses running on different tracks of a sand beach (from wet to dry) and on an asphalt road. *Equine Vet. J.* **2010**, *42*, 488–495. [[CrossRef](#)]
78. Ratzlaff, M.H.; Wilson, P.D.; Hutton, D.V.; Slinker, B.K. Relationships between hoof-acceleration patterns of galloping horses and dynamic properties of the track. *Am. J. Vet. Res.* **2005**, *66*, 589–595. [[CrossRef](#)]
79. Clanton, C.; Kobluk, C.; Robinson, R.A.; Gordon, B. Monitoring surface conditions of a Thoroughbred racetrack. *J. Am. Vet. Med. Assoc.* **1991**, *198*, 613–620.
80. Setterbo, J.J.; Fyhrie, P.B.; Hubbard, M.; Upadhyaya, S.K.; Stover, S.M. Dynamic properties of a dirt and a synthetic equine racetrack surface measured by a track-testing device. *Equine Vet. J.* **2013**, *45*, 25–30. [[CrossRef](#)]
81. Bertram, J.E.A.; Gutmann, A. Motions of the running horse and cheetah revisited: Fundamental mechanics of the transverse and rotary gallop. *J. R. Soc. Interface* **2009**, *6*, 549–559. [[CrossRef](#)]

82. Pfau, T.; Witte, T.H.; Wilson, A.M. Centre of mass movement and mechanical energy fluctuation during gallop locomotion in the Thoroughbred racehorse. *J. Exp. Biol.* **2006**, *209*, 3742–3757. [[CrossRef](#)] [[PubMed](#)]
83. Tabor, D. The physical meaning of indentation and scratch hardness. *Br. J. Appl. Phys.* **1956**, *7*, 159–166. [[CrossRef](#)]
84. Roepstorff, L.; Johnston, C.; Drevemo, S. The effect of shoeing on kinetics and kinematics during the stance phase. *Equine Vet. J.* **1999**, *31*, 279–285. [[CrossRef](#)] [[PubMed](#)]
85. Back, W.; van Schie, M.H.; Pol, J.N. Synthetic shoes attenuate hoof impact in the trotting warmblood horse. *Equine Comp. Exerc. Physiol.* **2006**, *3*, 143–151. [[CrossRef](#)]
86. Willemen, M.A.; Savelberg, H.H.C.M.; Barneveld, A. The effect of orthopaedic shoeing on the force exerted by the deep digital flexor tendon on the navicular bone in horses. *Equine Vet. J.* **1999**, *31*, 25–30. [[CrossRef](#)]
87. Huang, W.; Yaraghi, N.A.; Yang, W.; Velazquez-olivera, A.; Li, Z.; Ritchie, R.O.; Kisailus, D.; Stover, S.M.; Mckittrick, J. A natural energy absorbent polymer composite: The equine hoof wall. *Acta Biomater.* **2019**, *90*, 267–277. [[CrossRef](#)]
88. Roepstorff, L.; Johnston, C.; Drevemo, S. In vivo and in vitro heel expansion in relation to shoeing and frog pressure. *Equine Vet. J.* **2001**, *33*, 54–57. [[CrossRef](#)]
89. Hagen, J.; Hüppler, M.; Geiger, S.M.; Mäder, D.; Häfner, F.S. Modifying the Height of Horseshoes: Effects of Wedge Shoes, Studs, and Rocker Shoes on the Phalangeal Alignment, Pressure Distribution, and Hoof-Ground Contact During Motion. *J. Equine Vet. Sci.* **2017**, *53*, 8–18. [[CrossRef](#)]
90. Chateau, H.; Degueurce, C.; Denoix, J.-M. Effects of egg-bar shoes on the 3-dimensional kinematics of the distal forelimb in horses walking on a sand track. *Equine Vet. J.* **2006**, *38*, 377–382. [[CrossRef](#)]
91. Clayton, H.M.; Starke, S.D.; Merritt, J.S. Individual Limb Contributions to Centripetal Force Generation during Circular Trot. *Equine Vet. J.* **2014**, *46*, 38. [[CrossRef](#)]
92. Clayton, H.M. Comparison of the stride of trotting horses trimmed with a normal and a broken-back hoof axis. *Proc. Annu. Conv. Am. Assoc. Equine Pract.* **1987**, *33*, 289–298.